FROM IMAGERY TO MAP:

digital photogrammetric technologies

16th International Scientific and Technical Conference

Conference Proceedings

Organizer

Racurs
(Moscow, Russia)

Partner

OPSIS SYSTEM
(Kolkata, India)

Supported by

- **International** Society for Photogrammetry and Remote Sensing (ISPRS)
- State Space Corporation **ROSCOSMOS**
- **Russian** Society of Geodesy, Cartography and Land Management
- GIS-Association **Russia**

Dear colleagues!

We present to your attention the proceedings of the 16th International Scientific and Technical Conference "FROM IMAGERY TO MAP: digital photogrammetric technologies".

Technology develops most successfully when specialists exchange information freely; one of the most unique aspects of this conference is its international reach. Over its fifteen-year history, the conference has been held in thirteen countries sometimes far away of Russia and Europe.

Traditionally, the main topic of the conference is photogrammetric processing of aerial and satellite images. The related issues such as 3D modeling and new technologies do not go unheeded.

Undoubtedly, the proceedings will be useful and informative for you.

Sincerely yours,
the Scientific Committee of
the 16th International Scientific and Technical Conference
"FROM IMAGERY TO MAP: digital photogrammetric technologies"

16th International Scientific and Technical Conference
"FROM IMAGERY TO MAP: digital photogrammetric technologies"
November 14-17, 2016, Agra, India.

RACURS

2016

CONTENT

Photogrammetry and Cloud Technologies

Victor Adrov, Andrey Sechin, Racurs, Russia

Cloud technologies are getting more and more popular. This popularity is based primarily on convenience and commercial advantage. Cloud technologies allow cost savings and increase profit. We will consider, first of all, the various elements of cloud technologies from a technical point of view and the ability to use cloud technologies for photogrammetric processing. We illustrate the material with DPW PHOTOMOD deployment in the Amazon Elastic Compute Cloud (USA), CloudEO (Germany) and Rostelecom (Russia) clouds.

Cloud technology is a combination of different elements. One of these elements is a cloud data storage. Many of us make smartphone photos, and these photos are automatically uploaded to a cloud, making photos immediately available on other devices and computers and creating a safe backup. Microsoft has included Onedrive cloud storage in Windows 10. Apple's operating system is actively promoting iCloud not only for their devices. Other well known cloud storages are: Dropbox, Google Drive, Yandex Disk (Russia), Cloud of Mail. ru (Russia). There are dozens of different cloud storages, for personal or for corporate usage, free or paid. Companies that need their enterprise cloud data storage, can deploy their own clouds using OwnCloud, Pydio, NextCloud or other software solutions.

Cloud storage providers try to maximize the data access speed, but it is not always high enough. We have tested the access speed by downloading 1 GB file from Dropbox, one of the most popular solutions, using different Russian providers based in different Russian cities, as well as from London and Stockholm. The difference in tests between the slowest (Khabarovsk) and the fastest (London) accesses was more than 30 times. If such a cloud storage is necessary to hold large amounts of satellite or aerial imagery, such a solution is not suitable due to the low exchange rate from Russia. Probably the speed will increase in future as companies are beginning to widely implement the CDN (Content Delivery Network) technology to replicate data across multiple servers, and to provide the closest one to the user.

From the developer point of view the access to cloud data is different for different clouds. For example Yandex Disk uses the WebDAV access, and a so-called REST API, and Google Drive does not use WebDAV, and uses a different version of the REST API. Mail.ru also uses its own version of the REST API, and WebDAV (in test mode). Unfortunately unified software interface to various cloud data does not exist. It should be noted here that all cloud storages provide secure access to their data so that it is protected against unauthorized access.

Another element of cloud technologies is cloud computing. Currently, companies do not need to have powerful computing workstations or clusters, they can use virtual computers over the internet. Cloud computing is offered by many companies. Microsoft has Microsoft Azure - a cloud computing platform that provides Microsoft software and operating systems, and third party software and systems. Amazon offers a universal computing solution called Elastic Compute Cloud (EC2). Russian Rostelecom offers a Virtual Data Center and Storage that combines cloud storage with cloud computing. Cloud computing price usually starts from $5/month and can be hundreds of dollars per month depending on platform power. Virtual cloud "computers" usually have many CPU cores and even many computer nodes. If photogrammetric systems are to use the full processing power of these cloud computers, they have to support distributed computing.

Commercial operators of remote sensing satellite systems also have cloud technologies proposals. The American company Digital Globe offers partners to deploy their algorithms in the form of the so-called Docker containers and provides access to satellite images through REST API. In Europe German company CloudEO provides access to satellite imagery from their virtual cloud servers.

Our company has done several tests on different cloud platforms by running different automatic photogrammetric algorithms using PHOTOMOD software. We have tested Amazon EC2, CloudEO, Virtual Data Center from Rostelecom. We have

not tested the cloud from Digital Globe for two reasons: (a) there are technical problems with Docker container running PHOTOMOD, (b) there is no support of REST API in PHOTOMOD.

Let us proceed to the results of our tests. In the case of Amazon EC2 we have faced with a very low data upload speed from Russia (it was less than 600 kbytes/c). A mounth would be required to upload the 1.5TB project data. Upload and download times to/from the EC2 server are many times longer than the calculations times. We have used a virtual machine with the following parameters - 40 CPU cores, 160GB RAM, HDD 250GB + 100GB and had no problems running photogrammetric algorithms on PHOTOMOD DPW.

PHOTOMOD automatic algorithms also worked on CloudEO platform. In this case, we were faced with non-technical and organizational problems of data access and the absence of a network access to the software. We controlled DPW through the web browser.

The most comprehensive testing was done on Rostelecom cloud servers. For the testing purposes the following computing resources have been allocated: Number of CPU cores – 168 (2.6 GHz), 656 GB of RAM, disk space HDD 7000rpm - 12900GB, disk space HDD 15000rpm - 8000GB, the SSD disk space - 500GB. Upload and download speeds were up to 100 times higher than in the case of Amazon EC2, to upload the 1.5TB project 7.5 hours were required. We have run different photogrammetric algorithms - tie points measurements, dense surface models creation, orthorectification and ortho mosaic generation. In almost all calculations CPU load ranged from 80 to 100%, with small dependence on the HDD speed (7000rpm or 15,000 rpm). The RAM size was enough for all tasks. Orthorectification and ortho mosaic generation showed large sensitivity to the HDD speed. The time difference when using HDD 7000rpm vs 15000rpm was more than 1.5 times. The SSD storage size was insufficient to run the algorithm. Our tests on other hardware platforms show that SSD usage greatly increases the CPU load and reduces calculation time for these algorithms.

Our tests have shown that cloud computing can be successfully used for automatic photogrammetric calculations when virtual servers are combined with cloud storage. In case when the cloud storage is supplied separately from cloud computing servers DPW will need cloud storage API access functions and local data caching. An important factor of some algorithms is data access speed. Not all photogrammetric operations can be always done automatically. If one needs stereo processing (or stereo data control), the photogrammetric software should use the client-server model with a stereo capable remote client.

The savings of using cloud technologies in photogrammetry depend on the cloud storage and cloud computing prices. Another savings possibility in photogrammetric cloud processing can be based on the different price of satellite images when the user does not physically downloads them to his computer (Digital Globe proposal) and processes them in the cloud. However, this approach has several legal and organizational issues.

DPW software developers traditionally offered software licenses when the buyer becomes the full owner of the software product. Further development of cloud technologies and services will lead to a different business model when DPW will be offered as a SaaS (Software as a Service) or IaaS (Infrastructure as a Service) - that is as a cloud storage combined with the virtual cloud computer and the software for automated processing of satellite or aerial images.

Experiment and Technologic Small Spacecraft 'Aist-2D': First Results of On-Orbit Operation

Ravil Akhmetov, Evgeniy Kosmodemianskiy, Nikolay Stratilatov,
Anatoliy Raschupkin, Oleg Vlasenko and Alexandr Fedoseev
Joint-Stock Company 'Space Rocket Center 'Progress', Russia

Experiment and technologic small spacecraft (s/c) 'Aist-2D' was launched in April, 28, 2016 from spaceport 'Vostochniy' via rocket vehicle 'Souz-2-1a' and booster 'Volga' integrally with s/c 'Lomonosov' (developer – 'VNIIEM Corporation', JSC) and autonomous module of scientific and technologic apparatus 'Kontakt-Nanosputnik' (developer – University of Samara). 'Space Rocket Center 'Progress', JSC is the developer and operator of s/c 'Aist-2D'. It also provides manipulation of s/c, also reception and processing of received information.

The main aims of the s/c mission are developing and demonstration of new engineering solutions, testing and certification of objective sensors, scientific instruments, support systems and software for further use in JSC 'Space Rocket Center 'Progress' advanced development.

Payload also consists of a high resolution optic-electronic sensor 'Avrora', which provides Earth surface imagery acquisition in panchromatic and three narrow multispectral bands of visible spectrum range. The received information has some potential in the sphere of its practical application for define range of users.

Nowadays in-flight tests are being continued, procedures for limit characteristics of s/c are being developed and provided, such as on-board equipment power, controllability, transmitted information capacity via 's/c – Earth' channel, etc. Moreover, in order to design a modern s/c based on existent Aist-deck. but with high quality products acquisition, recommendations are being developed.

During s/c 'Aist-2D' in-flight tests potentials of high quality remotely sensed information via this type of s/c have been confirmed.

Procedures for methods optimization of imagery accuracy characteristics upgrading are being provided. Developing ways to implement received imagery in practice is also being processed. The possibility of swath extension via s/c rolling deflection (±45°) is being provided.

Certain activity considering implementation of remotely sensed information from s/c 'Aist-2D' is being made cooperatively with interested organizations and structures. It is aimed to be introduced to practical work of such users as Ministry of the Russian Federation for Civil Defense, Ministry of Agriculture, Federal Service for State Registration, Cadastre and Cartography, regional structures of the executive branch and commercial structures.

In the stage of the s/c development the s/c-deck principle has been used which provides building-up of s/c for different purposes with wide bevy of sensors among other scientific instruments. Further development of this project in the remote sensing area can help to produce series of small s/c with aim characteristics for high resolution, wide-coverage and stereo imaging.

Moorea Avatar – Physical Ecosystem Modeling of a Tropical Island

Prof. em. Dr-Ing. Dr.h.c. Armin Gruen
c/o Institute of Theoretical Physics, ETH Zurich, Switzerland

The global environment sustainability challenge

Human activities are affecting climate change and biodiversity loss on a planetary scale. The transition towards environmental sustainability, one of the defining challenge of our time, will require a far better understanding of complex social-ecological systems at local and national scales of management. To that end, a key research goal is to build functioning digital simulations, 'avatars', of model cities, islands and other objects to improve our ability to predict human and natural change especially at the scale of policy and management action.

Island Digital Ecosystem Avatars

Island systems are particularly attractive for sustainability science because they are tractable. Their geography provides a common boundary for biological and social networks, and sets clear limits on the species to inventory, ground cover to measure, organisms to count, and biosocial interactions to consider. Islands thus approximate idealized isolated ecosystems and represent rich sources of 'natural experiments'.

Moorea Avatar

The Moorea Island Digital Ecosystem Avatar (IDEA) project has been initiated in 2013 by a group of international researchers to build a virtual representation of Moorea Island. The main aim of the project is to model an entire ecosystem, observe the changes through it and be able to predict future changes reliably. The Moorea IDEA project incorporates observations, experiments, data, and theory across a coupled 3-D marine-terrestrial landscape to model, where physical, chemical, biological, and social processes interact to shape the island's phenotype. Moorea is a natural laboratory spanning marine and terrestrial environments that is constrained enough to be tractable, but sufficiently large (132 sq. Km) to contain all the elements of a complex socio-ecosystem, including a sizable human population (~ 17,000) (http://mooreaidea.org).

In order to generate the 3D physical model of the Island, multi-sensor data with varying accuracies, timestamps and spatial resolutions need to be processed and fused. High resolution optical satellite images (Pleiàdes), LIDAR data over land and water, existing DTMs, aerial film photography extracted and scanned from archives, underwater sonar measurements for modelling the bathymetry, underwater photogrammetry for monitoring the coral growth, UAV flights for accurate building reconstruction and recording of archaeological sites are among the data being processed in the project. This presentation describes the project in detail and addresses the processing methods and the problems encountered during the processing of multi-sensor and multi-resolution data. High resolution DSMs and orthoimages have already been generated using Pleiàdes images with 70 cm pan resolution acquired over Moorea and Tetiaroa in summer 2014. The images are tasked upon request and acquired in triplet mode, which provides three images from different angles for stereo processing with a time difference in the order of seconds. High resolution bathymetry data is available and will also been integrated into the generated DSM. The final physical 3D model, amended by landuse data and other semantic information will provide a presentation and a geospatial analysis platform to the project participants from many other disciplines.

Building on the Moorea Island Digital Ecosystem Avatar (IDEA) platform (http://mooreaidea.ethz.ch), our overall goal is to develop data-driven models of the spatio-temporal dynamics of all processes of relevance on land and in the sea. Advanced computational simulations will be developed.

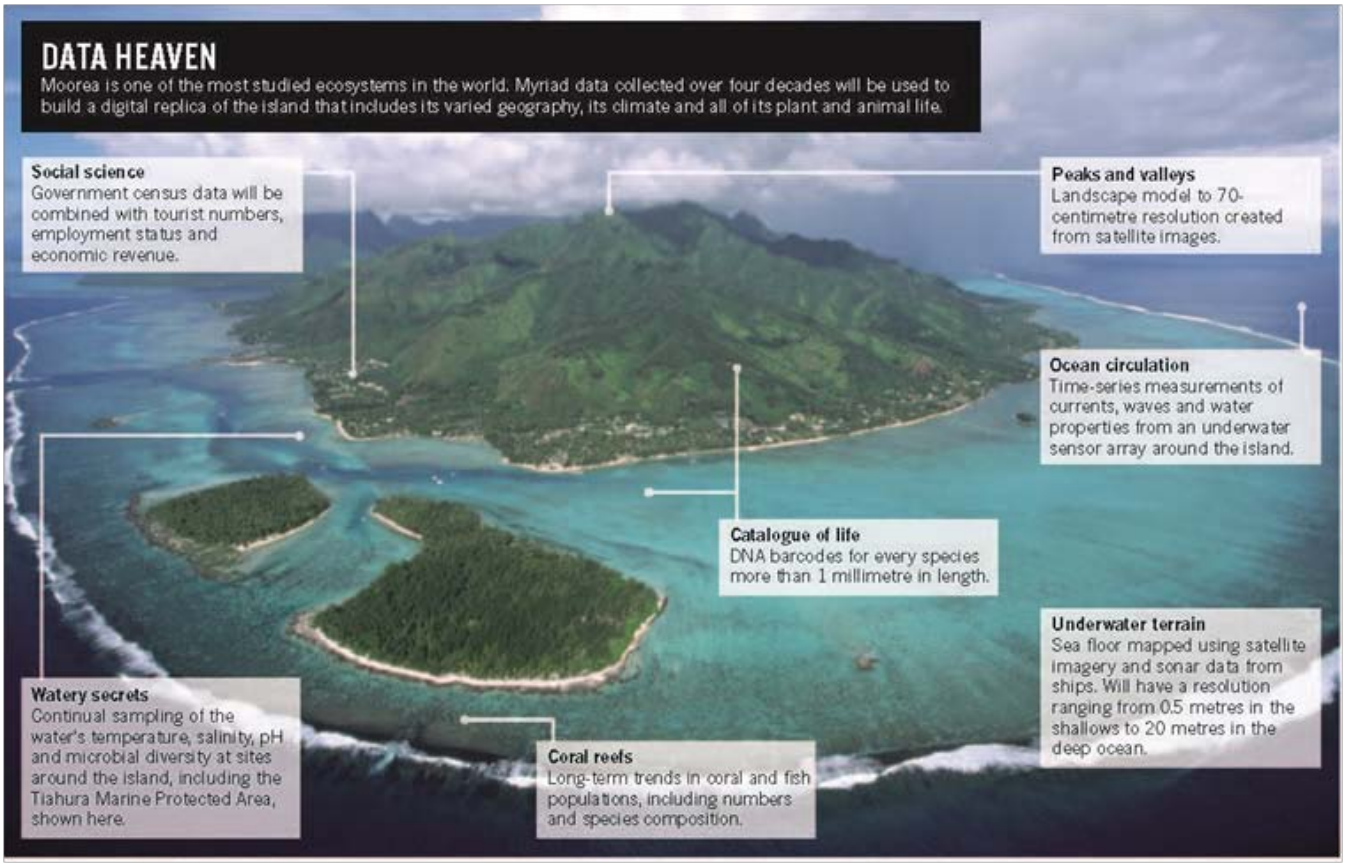

From: Daniel Cressey: Tropical paradise inspires virtual ecology lab. NATURE, Vol. 517, 15 January 2015

3D Modelling of IIT BHU Varanasi campus, using photogrammetric techniques on UAV captured data

Himanshu Nagrath[1], Biswajit Behera[1], Dr. Anurag Ohri[2]
1. Indshine Geoinformatics, India
2. Civil Engineering, IIT BHU Varanasi, India

Keywords: Aerial surveying, City 3D model, Photogrammetry, Ground Control Points

The 3D modelling of Indian Institute of Technology BHU is being carried out with the help of unmanned aerial vehicle. UAV is a quadcopter designed and fabricated in-house specifically for aerial surveying. The purpose of this project is to develop digital data for future infrastructure planning and drainage system designing of the institute. This paper reports about using modern techniques of terrestrial and aerial photogrammetry to derive a photorealistic 3D model of campus. The accuracy of model is improved by using control points collected using DGPS and Total Station. Accuracy of model is tested using various DGPS check points in the site. The developed 3D model can be used as prototype for learning city modelling and planning.

3D Modeling of the Vishwanath Temple, Varanasi Using Close Range Digital Photogrammetry

Anurag Ohri, Manish Sahu, Department of Civil Engineering, IIT(BHU), Varanasi, India

Keywords: Digital Photogrammetry, Aerial and Terrestrial Photography, Control points, Heritage Building

The Vishwanath Temple in Banaras Hindu University is the highly visited religious and tourist place of Varanasi. Well-known for their structural and surface complexity, temple constitute a great challenge to any attempt towards precise and detailed 3D measurements and modeling. This paper reports about a project using modern techniques of terrestrial and aerial photogrammetry to derive a photorealistic 3D model of Temple. The accuracy of model is improved by using control points collected using DGPS and Total Station. Accuracy of model is tested by using various GCP in the site. This project is important to preserve our cultural heritage by documenting the various buildings of cultural and religious importance.

SIIS
SI Imaging Services

Satellite imagery

40 cm resolution product
We can zoom in to look at people visiting Barra Olympic Park.

Big picture with KOMPSAT

Barra Olympic Park in Brazil taken
by KOMPSAT-3A on August 13th, 2016

CONTACT

SI Imaging Services
Satrec Initiative Group

441, Expo-ro, Yuseong gu, Daejeon,
34501, Republic of Korea

sales@si-imaging.com
+82-70-7805-0372

www.si-imaging.com

Mapping the world

Stay informed with *GIM International* - anytime, anywhere

GIM International, the independent and high-quality information source for the geomatics industry, focuses on worldwide issues to bring you the latest insights and developments in both technology and management.

- Topical overviews
- News and developments
- Expert opinions
- Technology

Sign up for your free subscription to the online magazine and weekly newsletter today!

www.gim-international.com

GIM
INTERNATIONAL

geomares

3D Photogrammetry and 3D cartography

Andrey Sechin, Victor Adrov, Racurs, Russia

In the recent years there are a lot of talks on 3D maps, 3D GIS, 3D cartography, 3D city models. In this paper we consider the methods of providing metrical 3D information for such maps and models. We do not consider 3D models that have nice visualization properties but poor accuracy.

The main source of metrically accurate 3D coordinates is photogrammetry and LiDAR technologies.

Traditional Maps

Traditional paper maps and digital models are 2D or 2.5D. The third coordinate on traditional paper maps is shown by contour lines. Contour lines on a map are curves produced from connecting points of equal elevation. Closely placed contour lines represent steep slopes. One needs some practice and understating to read maps with contours. Contour lines have rather loose accuracy requirements (usually accuracy is 1/3 of a contour interval). Maps can also have spot heights – the dots with the given altitude. Now computer technologies have replaced paper maps with GISes (Geographic Information Systems) that can display maps on a computer screen. Height coordinates (or elevations) in such systems are stored as DTM (Digital Terrain Model) – that is a raster type data – a grid of equally spaced cells with height values. These height values have vegetation, buildings and man made features removed. DTM can be displayed with height-based coloring, as contours or even as a 3D shaded model. These models are called 2.5D because they are constructed by projecting real 3D coordinates to a 2D plane. In 2.5D models there is only one Z (height) value for the given XY coordinates.

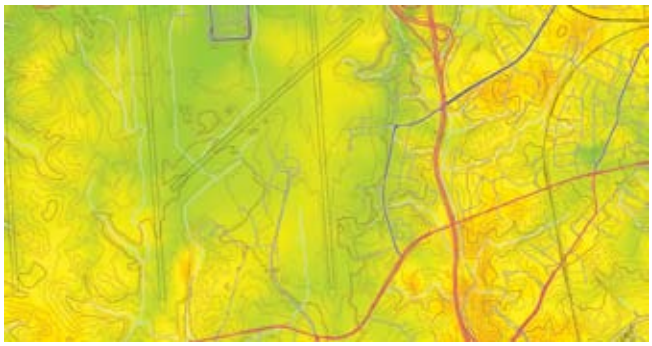

Vector 3D Maps

3D coordinates can be obtained from photogrammetric processing. In photogrammetry aerial or satellite images blocks are used as input data. DPW (Digital Photogrammetric Workstations) can automatically calculate DTM after the so called block adjustment. In DPW one can combine a couple of images (stereopair) and draw accurate 3D vectors manually, describing houses, roads, bridges and assigning codes or other metadata to the drawn objects. Our estimates show that one human operator can draw a city area of 0.2-0.3 km2 per day when the aerial images GSD (Ground Sample Distance or image pixel size) is 7-10 cm. This manual technique produces fine city vector models that can be combined with photos made from earth level by consumer cameras, or with predefined textures. These models do not require a lot of storage and can be used in 3D GISes. An example of such a model is shown below.

LiDAR point clouds

Light detection and ranging (LiDAR) mapping is a method of generating precise, directly georeferenced point clouds - very dense and accurate elevation data across landscapes. LiDAR consists of a laser, scanning system, photodetector and receiver electronics, position and navigation systems [1]. LiDAR measures the time to reflect the light from the land surface and transforms it to the distance. These distances are converted into georeferenced 3D points using navigation GPS/IMU data. Typically, LiDAR-derived elevations have absolute accuracies of about 10 to 20 cm and

have density of several points per m2. To create a 3D point cloud of a landscape LiDAR is attached to a plane during flight (airborne LiDAR). LiDAR technology is not new, laser-based remote sensing began in the 1970s. LiDAR point clouds can be the source for making DTM's. Reflected laser light provides not only distance. One laser beam can have multiple reflections or returns (from top of trees, low vegetation, ground). This additional information can be used to classify LiDAR points. We will speak about point classification later.

3D Point Clouds from Photogrammetry

Recent development of dense correlation methods, especially SGM (Semi Global Matching) [3] algorithm can produce dense 3D point clouds from aerial or satellite images. The density and accuracy of calculated points is about GSD and can be even better than in LiDAR technology (it depends on flying height and camera). These dense matching algorithms handle surface occlusions and height discontinuities and can calculate 3D points on roofs and walls of buildings (aerial city images) and on other objects. High images overlap 80-90% (forward) and 60-70% (side) is required for such modeling. Many aerial camera manufactures now produce cameras that provide simultaneous combined nadir and oblique images. Such cameras are preferable for city modeling. Complex buildings can be represented as 3D point clouds. 3D points from dense matching are assigned colors from original images for visualization.

What is it all for

3D views of Earth surface, cities, landscapes, etc made from 3D points with color are very realistic. 3D information is useful for many tasks – for disaster management (flood, fire, earthquake etc.), for radio waves propagation, for navigation, for urban planning, for 3D cadastre, for lightning simulations, for forest management, for propagation of noise simulation, for visualization and many other things. Different tasks require different 3D data. There are many working examples of 3D GIS systems, but still there are no standards for 3D mapping and cartography. If we consider 3D point clouds – they are good for visualization, but give little help for navigation and other tasks. In 3D cartography, 3D GIS maps are constructed from points, lines, polygons, symbols, colors, patterns. Different colors, point sizes, or line thickness can denote different values. These map elements are combined into objects – roads, buildings, lakes, rivers, mountains. Objects are assigned codes or names – building numbers, road names, etc. Let us estimate if a map can be constructed only from 3D points (with assigned colors and codes).

We will take India as an example and suppose we have 3D point cloud describing all India with point spacing of 50 cm. The total India area is 3,287,263 km2. This will require more than 1013 points. Each point has at least a height (16 bytes), color (24 bytes), and an object index (8 bytes) – we simplify the estimates and assume that points are located in the nodes of regular XY grid. That gives us about 5*1016 bytes of information or 50 pentabytes, or 50000 terabytes of information. To store the single copy of this information one needs about 8000 high capacity hdds. To make such storage reliable the data must be stored with redundancy. The spacing of 50 cm is not enough for cities. In cities 10 cm accuracy and spacing may be required. This leads us to the need of data storage close to world record storage solutions. Thus 3D point clouds must be converted to something requiring less data storage.

As it was mentioned before LiDAR technology can classify 3D points into buildings, vegetatation, etc. There are now semi-automatic algorithms to segment building roofs from 3D information and additional LiDAR data (reflection number) or image color or infrared channel. These algorithms still need some manual post processing to fix

incorrectly segmented objects.

Many investigations are now carried out to segment 3D point clouds into buildings, buildings facades, road network, vehicles and pedestrians (to be excluded from the results), lampposts, trees, vegetation, etc. Different approaches and algorithms are proposed, but there is still no automatic reliable methods for such segmentation [2],[4].

Up to now the best 3D information that can be used in 3D GIS, 3D cartography, 3D maps is a set of vector 3D objects vectorized manually in stereo.

Conclusion

Current advances in photogrammetry (dense matching) can produce metrically accurate 3D point clouds that are in many cases more accurate and dense then LIDAR points. These (or LiDAR) points can be assigned colors taken from aerial or satellite images, this allows to display realistic 3D views of Earth surfaces. Point clouds require a lot of storage and cannot be directly used for tasks requiring 3D information. Different algorithms to segment 3D point clouds and convert them into vector primitives (lines, polygons, surfaces) or vector objects (roads, buildings, bridges, trees, etc) are still under development. The best 3D model creation technique is still based on manual stereo vectorization that is time consuming and expansive. The new algorithms that are under development will convert 3D points into 3D models similar to the models produced by stereo vectorization. Codes, building numbers, names are still to be assigned manually in GIS.

References

1. Baltsavias, E.P.Airborne laser scanning: existing systems and firms and other resources ISPRS Journal of Photogrammetry & Remote sensing, (1999), pp.164-198

2. Boyko, A. and Funkhouser, T., Extracting roads from dense point clouds in large scale urban environment. ISPRS J Photogrammetry & Remote Sensing 66(6), (2011),pp. 2–12.

3. Hirschmuller, H.: Stereo processing by semi-global matching and mutual information. IEEE Transactions on Pattern Analysis and Machine Intelligence 30 (2008) 328–341

4. Shapovalov, R., Velizhev, A. and Barinova, O., Non associative markov networks for 3D point cloud classification. ISPRS Archives, (2010).

UAS data processing retrospective

Alexey Smirnov, Racurs, Russia

Aerial topography survey of the Earth's surface has long history. People use pigeons, kites, balloons with mounted camera for years. During the World War Two unmanned aerial systems (UAS) improved to a miniature aircraft used for military tasks. Today, UAS is officially used along with manned civil aviation in many countries.

Professional interest in UAS to obtain spatial data emerged in the early 2000s. At the present time many companies offer UAS survey due to affordability, high productivity, and efficiency.

Image processing operations were performed on mechanical and analytical stereocomparators, stereoautographs, stereometrs, stereoprojectors and multiplexes before digital era. Modern digital photogrammetric systems (DPS) include tools adapted for UAS data processing.

The flip side of UAS today is to usage of "shop" cheap drones and primitive methods of data processing for topographic tasks where accuracy at each stage of processing and quality control of the output materials are the highly important.

Typical products from UAS data photogrammetric processing are orthophoto, digital terrain model, digital surface model and 3D models. Professional quality control of results is possible only with a reporting system at each stage, and stereo window.

The report will provide an overview of the unmanned systems design and development over the past 10 years. The overwiev is the basis for vehicles classification on their adaptability for monitoring tasks or accurate measurement for large-scale mapping purposes.

The report will provide the analysis of digital photogrammetric systems functionality. Analysis of UAS aerial survey is shown particular geometrical characteristics of images. It is possible to determine the necessary set of tools adapted for modern DPS and to specify the development of software and hardware systems.

UAS and data processing applications are evolving towards to full automation, cloud solutions, automated storage and data analysis. The market will be providing a full set of services using UAS with deep orientation on a particular organization needs.

In the future, automation and full visualization of three-dimensional virtual space will allow to carry out UAS image processing and analyze the results. Mapping, urban planning, and industrial modeling based on the output photogrammetric products will be carried out in the presence of the virtual mode.

Delineation of Japanese encephalitis disease risk zone area in district Gorakhpur, Using an AHP Approach

Shipra Verma, Motilal Nehru National Institute of Technology, India

The health assessment and management requires precise quantitative assessment based on scientific principle and modern techniques. In the present study, Japanese encephalitis (JE) risk zone area are delineated using remote sensing, geographical information system (GIS) and decision making techniques in Gorakhpur district, Uttar Pradesh. The method makes it possible for one to deal systematically, includes the analytical hierarchical process (AHP) as a special case. The AHP are used to determine the weights of various themes and their classes for identifying the disease risk areas. It has been concluded that about 946.44 km2 areas are in severe condition in 27.19%, of total area. However, the area having very poor and poor are about 239 km2 and 160.44 km2 which is about 6.99% and 4.61% of the study area. The area having high and moderate risk is about, 985.616 km2 and 1152.198 km2, with 28.29%, to 33.08%, respectively. The JE risk zone map finally verified using the JE disease death of year 2009 and the result was found satisfactory.

Keywords: JE, GIS, AHP, risk zone.

1. Introduction

Health information and statistics are important for planning, monitoring and improvement of services for the health of populations (Murray et al., 2003). These are essential for policy-makers and programme planners to inform their decisions about what actions to take and what services to provide in order to improve the health of the populations they serve (Raban et al., 2008). Japanese encephalitis (JE) is a mosquito borne disease caused by a neurotropic flavivirus, named Japanese encephalitis virus (JEV).

The viral encephalitis was reported in July through November 2005 in Gorakhpur. It was the longest and most severe epidemic in three decades. As reported, 5,737 people were affected in seven districts of Eastern Uttar Pradesh and 1,344 people died (WHO, 2005; Srivastava et al., 2008).

GIS serves as a useful tool for the integration of the data gathered through analysis and manipulation, in the form of maps for the study. In decision support system, just GIS are not sufficient (Jankowaski 1995). The disease risk planning and management requires a model for the district to assess the disease involving factors. The conceptual model is prepared using Analytical Hierarchy Process (AHP), which is most suitable for screening high risk-zone areas, using weighted analysis steps.

xThe main aim of this study is to determine the areas that are responsible for the JE disease growth. To delineate these risk-zone areas, including the above responsible factors, a decision needs to be taken. This approach should be developed by using some decision making process. AHP is a MCDM theory proposed by Saaty (1987), which is used in GIS applications due to its ability of dealing with multiple factors. MCDM is used to solve various site selection problems (Jun 2000, Albayark et al., 2003).

2. Study Area:

The site for this study was the Gorakhpur district (figure. 1) Uttar Pradesh the state of India. It has an area of 3483.8 sq. km. The district lies between lat. 26°13′N and 27°29′N and long. 83°05′E and 83°56 ′E. Gorakhpur occupies the north eastern corner of the state of Uttar Pradesh, and is located to the north of the river Ghaghra.

Gorakhpur districts corresponds to 7 tehsil and 19 blocks.

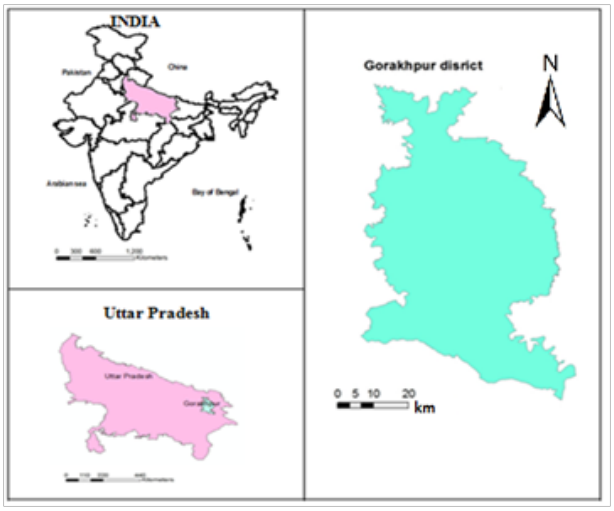

Figure 1: Study Area: India, State of Uttar Pradesh, and District Gorakhpur

DATA SHEET

DigitalGlobe™

WorldView-4

Introducing WorldView-4, a multispectral, high-resolution commercial satellite. Operating at an expected altitude of 617 km in coordination with WorldView-3, WorldView-4 provides 31 cm panchromatic resolution, and 1.24 m multi-spectral resolution. With WorldView-4 joining WorldView-3 in the DigitalGlobe constellation, our total constellation has the capability to image a location an average of 4.5 times/day at 1m GSD or less

Features

- Very high-resolution
  - Panchromatic 31 cm
  - Visible & near-infrared 1.24 m
- Industry-leading geolocation accuracy
- High capacity in various collection modes
- Bi-directional scanning
- Rapid retargeting using Control Moment Gyros (>2x faster than any competitor) resulting in superior area and point target collection capability
- Direct Access tasking from and image transmission to customer sites
- Daily revisits

Benefits

- Simultaneous, high resolution, multi-spectral imagery
- Large area single-pass (synoptic) collection eliminates temporal variations
- Precision geo-location possible without ground control points
- Global capacity of 680,000 km² per day

WorldView-4 artist rendering

3. Spatial Multi Criteria Decision Making (SMCDM)

It is a process to combines and transforms geographical data into a decision (Malczewski 1999). The choice of criteria, as a geographical point of view, is integrated in the GIS environment (Jankowski, 1995; Malczewski, 1996). Spatial multi-criteria decision problems typically involve a set of geographically-defined alternatives (events), from which a choice of one or more alternatives is made, with respect to a given set of evaluation criteria.

It is important to prepare a model for JE disease of the district to assess the areas that were highly affected or are in low in condition. The methodology is prepared using AHP, for screening high-risk disease prone areas, using weighted analysis.

AHP uses a fundamental scale that consists of nine points, which are absolute numbers to express individual judgment (Table 1).

Intensity of importance on an absolute scale	Definition	Explanation
1	Equal importance	Two activities contribute equally to the objective
3	Moderate importance of one over another	Experience and judgment strongly favor one activities to over another
5	Essential or strong importance	Experience and judgment strongly favor one activities to over another
7	Very strong importance	An activity is strongly favored and its dominance demonstrated in practice
9	Extreme importance	The evidence favoring one activity over another is of the highest possible order of affirmation
2,4,6,8	Intermediate values between the two adjacent judgments	When compromise is needed

Table 1 Saaty's 1-9 scale of relative importance

Based on the properties of reciprocal matrices, the Consistency Ratio (CR) can be calculated. The level of consistency ratio CR> 0.1 indicates that a pair-wise comparison is acceptable. Saaty (1980) suggests that if CR is smaller than 0.10, then the degree of consistency is fairly acceptable.

4. Material and Methods

The following are steps to develop a model for JE disease using AHP methods are illustrating in Figure 2.

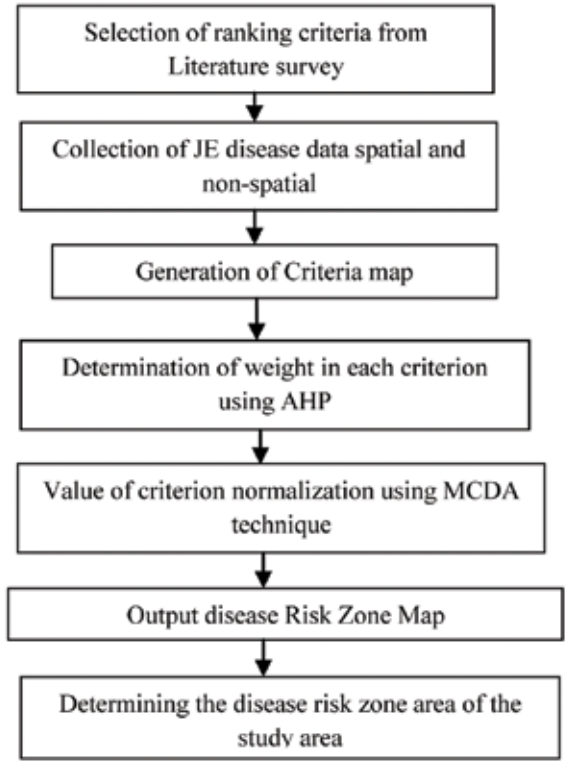

Figure 2: The Methodology for Generating JE Disease Risk Zone Areas

Figure 2 presents the analytical flowchart, step by step. The first part represents the selection of a study area, which includes health problems related to the JE disease from literature review. The next step is data collection and integration in the GIS environment,

4.1 Steps For Developing Risk Zone Area Of JE Disease

For accessing the spatial integration of factors in year 2009 which were responsible for spreading the disease, a common methodology could be to develop the related spatial databases regarding environmental conditions and socioeconomic conditions.

The generated spatial parameter like water area, paddy crop, number of pig population, land surface temperature, number of hospitals, soil map and the affected population disease data set have been prepared using a suitable spatial analytical

GeoConnexion

The Online Pack: Unbeatable Value

Just £1 a month

Join today!

Unlimited access to Online News, Comment, Features Sections and Archive plus Monthly eNewsletter packed with the Latest News and what's on in the **Geospatial Industry**

Join today for only £1 a month

Topics covered:

- ✔ 3D Visualisation/Modelling
- ✔ Addressing Technology
- ✔ Aerial Imagery/Photography
- ✔ Asset Management
- ✔ Bathymetry
- ✔ Big Data
- ✔ Business Geographics/ Analytics
- ✔ Cadastral Mapping
- ✔ Cartography
- ✔ Climate Change
- ✔ Computing in the Cloud
- ✔ Crime Mapping/ Modelling
- ✔ Data Capture/Collection
- ✔ DEM- Digital Elevation Model
- ✔ DGPS - Differential GPS
- ✔ Digital City Models
- ✔ Digital Mapping
- ✔ Digital Rights Management
- ✔ Disaster Management/ Monitoring
- ✔ DSM - Digital Surface Model
- ✔ DTM - Digital Terrain Model
- ✔ Dynamic Mapping
- ✔ Earth Observation
- ✔ Emergency Services
- ✔ ENC - Electronic Navigation Chart
- ✔ Environmental Monitoring
- ✔ Galileo
- ✔ Geo-ICT
- ✔ Geodesy
- ✔ Georeferencing
- ✔ Geosciences
- ✔ Geospatial Image Processing
- ✔ GIS
- ✔ GIS in Agriculture & Forestry
- ✔ GLONASS
- ✔ GMES
- ✔ GNSS
- ✔ GPS
- ✔ GSDI
- ✔ Hardware
- ✔ Hydrography
- ✔ Hyperspectral Imaging
- ✔ Image Analysis
- ✔ INSPIRE
- ✔ Integration
- ✔ Interoperability & Open Standards
- ✔ Land Information Systems
- ✔ Laser Scanning
- ✔ LBS
- ✔ LiDAR
- ✔ Mapping Software
- ✔ Marine Tracking & Navigation
- ✔ Mobile GIS/Mapping
- ✔ Municipal GIS
- ✔ Navigation
- ✔ Network Topology
- ✔ NSDI
- ✔ Open GIS
- ✔ Photogrammetric
- ✔ Photogrammetry
- ✔ Point Clouds
- ✔ Property Information Systems
- ✔ Radio Navigation
- ✔ Remote Sensing
- ✔ Risk Management
- ✔ RTK (Real Time Kinematic) Surveying
- ✔ Satellite Imagery/Navigation
- ✔ Scanning Technology
- ✔ SDI - Spatial Data Infrastructures
- ✔ Smart Grids
- ✔ Software
- ✔ Surveying Instrumentation
- ✔ Surveying Technology Sensor
- ✔ Telematics
- ✔ Topographic Mapping
- ✔ Total Station
- ✔ Tracking & Route Planning
- ✔ Transport
- ✔ Utilities GIS
- ✔ Vehicle Tracking & Navigation
- ✔ VRS - Virtual Reference Station
- ✔ Web Mapping

Sectors covered:

- ✔ Aerospace
- ✔ Agriculture
- ✔ Archaeology & Heritage
- ✔ Architecture
- ✔ Biosecurity
- ✔ Business Security/Service
- ✔ Central/Local/Regional Government
- ✔ Construction
- ✔ Consulting Services
- ✔ Cyber Security
- ✔ Defence
- ✔ Education
- ✔ Emergency Services
- ✔ Energy Utility
- ✔ Engineering
- ✔ Environmental Management
- ✔ Environmental Monitoring
- ✔ Financial Services
- ✔ Fisheries
- ✔ Forestry Management
- ✔ Geosciences
- ✔ Healthcare
- ✔ Infrastructure Protection
- ✔ Insurance
- ✔ Manufacturing
- ✔ Marine
- ✔ Military
- ✔ Mining
- ✔ Natural Resource Management
- ✔ Oil & Gas
- ✔ Property
- ✔ Public Safety/Works
- ✔ Retail
- ✔ Shipping
- ✔ Software Development
- ✔ Technical Services
- ✔ Telecommunications
- ✔ Tourism/Travel
- ✔ Training
- ✔ Transport
- ✔ Utilities (Energy & Water)

Subscribe and stay ahead of the game!
The content that you can trust

Sign up at geoconnexion.com/membership

technique. The database has created and related maps were digitized and rasterized accordingly. In this study following steps are used to evaluate JE risk zone blocks/zone There are four integrated steps to produce risk zone map of JE disease, and these are listed as follows:

- Collection, preparation, and integration of spatial and non-spatial database in the GIS environment
- Assigning weight to the parameter involved
- Generating risk zone JE disease map
- Determining the judgment

The detailed framework is shown in Figure 3.

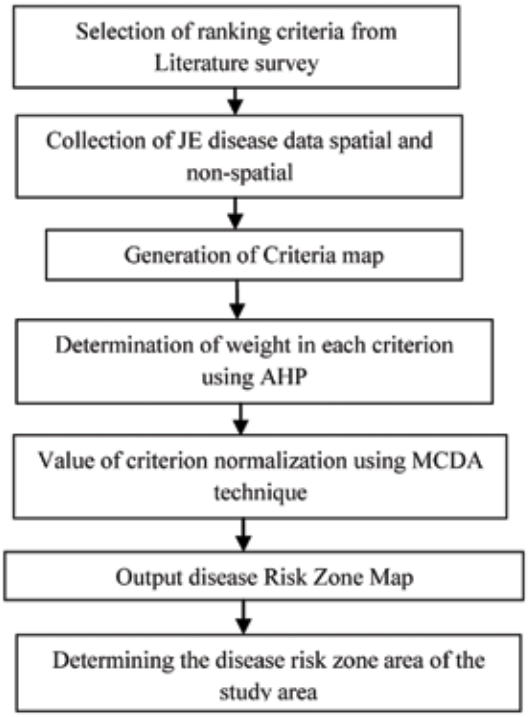

Figure 3: Flow chart of steps to follow for modeling JE disease risk zone site in Gorakhpur District.

AHP is applied to incorporate the decision by the judgment of environment factors environment factors, which are responsible for disease growth and preferences by using the AHP method.

Figure. 3 explains the workflow using AHP. ArcGIS 10 is used to combine the spatial data and is run in the AHP model to generate the disease risk map with a suitable index model technique along with a validated JE disease pattern map. The criteria maps are standardized with the relative importance of the class of each criterion. The final step involved in AHP is the aggregation of the relative weights obtained at each level of the hierarchy, to calculate the disease risk zone area. The output is developed for identifying the risk area of the disease in the entire district.

The final part deals with the recommendations of the public health department.

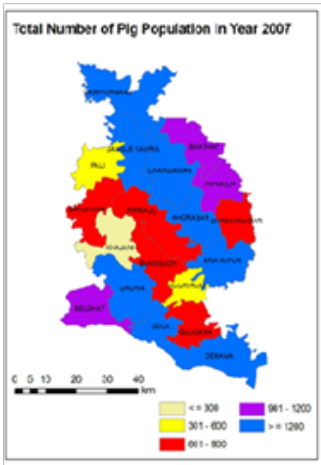

Figure 4: Pig Population Map for Year 2007

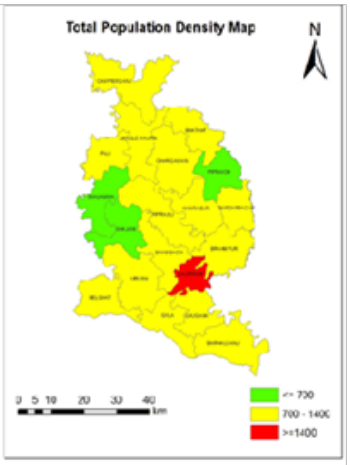

Figure 5: Total Population Density in Blocks

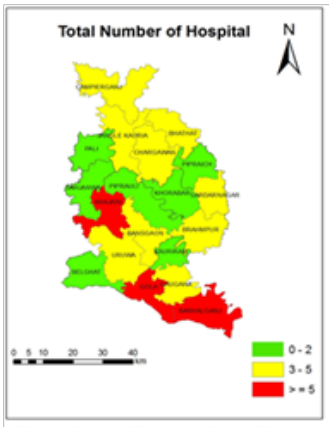

Figure 6: Number of Hospitals in Blocks of District

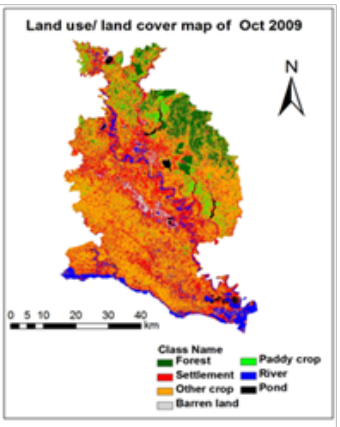

Figure 7: Land use land cover map of Oct 2009

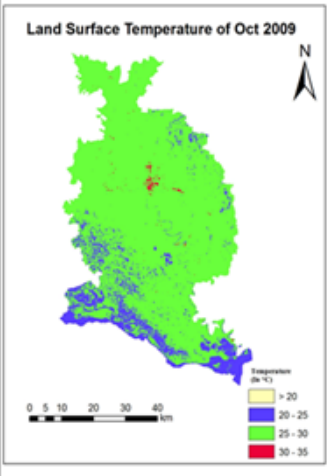

Figure 8: LST map of Oct 2009

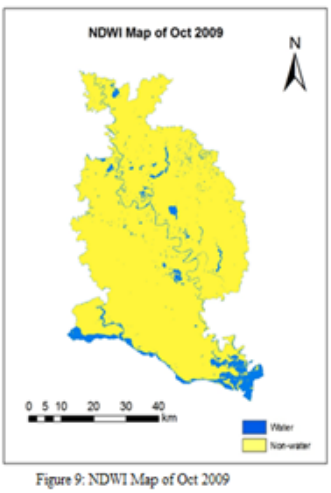

Figure 9: NDWI Map of Oct 2009

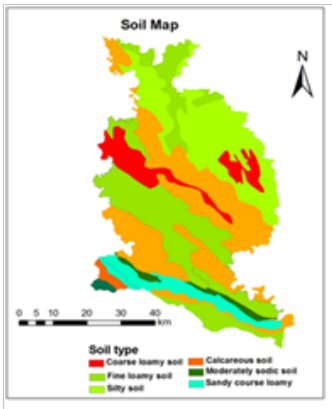

Figure 10: Soil Map of Gorakhpur District

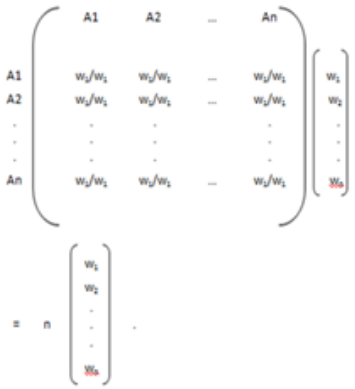

Figure 11: Digrammatic representation of pair wise matrix weighted model (Saaty, 1999)

4.2.2 Generation of pair-wise comparison matrices

The relative important values are determined with Saaty's 1 to 9 scale (table 8.1), where a score of 1 represents equal importance between the two themes, and a score of 9 indicates an extreme importance of one theme as compared to the other (Saaty1999).

The thematic maps are rasterized into a pair-wise matrix at individual level. This is shown in table 2.

Table 2 captures the idea of uncertainty in judgments through the principal Eigen value and the consistency index (Saaty 2004). Saaty gave a measure of consistency (using maximum-based criteria), called Consistency Index (CI), which is represented by the following equation (1):

$$C=(\lambda max-n)/(n-1) \quad \text{eq..(1)}$$

Here, λmax is the largest Eigen value of the pair-wise comparison matrix and n is the number of classes. Consistency Ratio (CR) is the measure of consistency of the pair-wise comparison matrix, and is represented by the following equation (2):

$$CR= CI/RI \quad \text{eq..(2)}$$

Here, RI is the Ratio Index. The value of RI for different n values is given in table 3.

PHOTOMOD

Digital photogrammetric system

Spatial aerial triangulation

Digital terrain models

2D and 3D-vectorization

Orthorectification and mosaic creation

Map making

3D-modeling

RACURS

LOOKING FOR INFORMATION ON...

Stay informed with GIS Resources
- anytime, anywhere

Information is delivered via all-new print and digital magazine published quatelry, a weekly eNewsletter and a stand-alone website

GIS Resources
A Knowledge Archive...

Sign up for free subscription to the digital magazine and weekly newsletter today!

www.gisresources.com

Table 2:Pair-wise comparison matrix comprises the related maps of various thematic layers and their corresponding classes.

Theme	Various Classes							CR/ Weight
Pig population	<690	691-1400	>1400	-	-	-	-	0.09/ 18.39
Weight	61.96	22.43	15.60	-	-	-	-	
Block wise Total Population	>1400	1401-700	<700	-	-	-	-	0.03/12.04
Weight	61.94	9.64	28.42	-	-	-	-	
Total Hospital	0-3	3-5	>5	-	-	-	-	0.09/10.05
Weight	26.90	39.95	8.14	-	-	-	-	
Landuse classes	Paddy crop	Other crop	Settlement	Water	Forest	Barren land	Pond	0.04/24.03
Weight	21.09	7.33	13.72	13.46	16.91	24.93	2.56	
Land surface Temperature	>28	28-27	27-26	26-25	<25	-	-	0.08/7.4
Weight	22.87	11.53	13.98	24.54	14.59	-	-	
NDWI Map	Water	Non-water	-	-	-	-	-	0.00/16.13
Weight	1	2						
Soil Map	Fine loamy	Coarse Loamy	Sandy	Calcareous	Sodic soil			0.007/11.95
Weight	35.40	13.05	32.60	12.27	6.67	-	-	

If the value of CR is less than or equal to 0.1, the inconsistency is acceptable. If CR is greater than 10 percent, it needs to revise the subjective judgment. CR for a pair-wise comparison matrix shown in table 2 is 0.09:

To obtain the weighted matrix for the study area in each block, each column of the matrix's weight is multiplied by the normalized value of each factor. To determine the final relative priorities, add the all value of factors and obtain a higher value of the weight to give the priority by itself.

The Saaty's scale is used to define the ratio index value in n series data, which is illustrated in table 3:

Table 3: Saaty's ratio index for different value of n.

N	1	2	3	4	5	6	7	8	9	10
RI	0	0	0.58	0.89	1.12	1.24	1.32	1.41	1.45	1.49

The generated weight matrix in between all the thematic maps from table 8.2 pair-wise comparison matrix is shown in table 4:

Table 4: Pair wise comparison matrix in generated thematic maps

	Total Hospital Map	Pig population Map	Landuse Map	Total Population Map	NDWI Map	Soil Map	Temperature Map
Total Hospital Map	1	1/3	¼	1/6	3	4	2
Pig population Map	3	1	½	5	8	½	4
Land use Map	4	2	1	6	9	3	7
Total Population Map	6	1/5	1/6	1	1/4	½	3
NDWI Map	1/3	1/8	1/9	4	1	8	1/5
Soil Map	1/4	2	1/3	2	8	1	½
Land surface Temperature	1/2	1/4	1/7	1/3	5	2	1

4.3 Ranking classes for various parameters

The occurrence and spread of disease in any area depends upon various factors, such as topography, rainfall, temperature, sanitation in concern for the JE disease response. Spatial analysis refers to the "ability to manipulate spatial data into different forms and extract additional meaning as a result" (Bailey. 1994, Cromley, 2003). The study is based on the disease environmental factor for 2009, by using remote sensing and GIS technique. The normalized matrix value is form in and explained in table 5:

Table 5: Normalized matrix value index

	Pig population Map	Total Population Map	Total Hospital Map	Landuse Map	Temperature Map	NDWI Map	Soil Map
Pig population Map	0.1077	0.3586	0.1925	0.3218	0.2254	0.3243	0.0112
Total Population Map	0.0359	0.1195	0.1925	0.2682	0.1127	0.1946	0.0260
Total Hospital Map	0.0359	0.0398	0.0642	0.0134	0.0141	0.2595	0.2342
Landuse Map	0.0359	0.0239	0.2567	0.0536	0.3944	0.0108	0.3123
Temperature Map	0.0180	0.0598	0.2567	0.0077	0.0563	0.1297	0.0260
NDWI Map	0.0215	0.0398	0.0160	0.3218	0.0282	0.0649	0.3123
Soil Map	0.7540	0.3586	0.0214	0.0134	0.1690	0.0162	0.0781

An AHP-based methodology supports the relative importance of various thematic layers and their corresponding classes. An impact on JE has been used to evaluate risk zone for the disease. Table 5 represents the weight of each thematic layer.

4.4 Overlay analysis to find JE Risk Zone Area (RZA) for JE

The risk zone map is computed by a weighted linear combination method (Malczewski 1999; Machiwal et. al., 2011), and is given by:

$$RZA = \sum_{i=1}^{n} W_i \int i$$

The disease probability area evaluated by the weighted linear combination of these weights is shown in Figure 12:

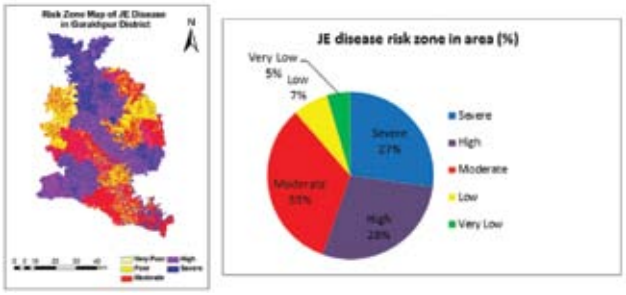

Figure 12: JE disease risk zone area map and distribution of JE disease Risk Zone area.

In this study, AHP technique supports the various thematic layers and their corresponding classes which affect JE disease and generate the most probable JE disease risk area. Results indicated that only 946.44 km2 areas are in severe condition, 985.616 km2 in high risk, 1152.198 km2 is in moderate and the areas in 239 km2 and 160.44 km2 in poor and very poor. In this, the contribution of the GIS was considered not only as a method for data gathering but also as the tool for mapping the result. A composite overlay map was visualized in the GIS that reflects the weights for criteria obtained from the MCDM module.

This gives a realistic JE disease risk zone area map of the study area, which can now be used for health planning and development with a high degree of confidence. Based on the result of this study, concerned decision makers can formulate the model to justify the JE disease area. To this end, a study was carried out to delineate JE disease risk zone area in the Gorakhpur district of Uttar Pradesh (India) using a multi-parametric approach by remote sensing (RS) and GIS techniques. Remote sensing satellite imagery (Landsat TM), SOI topographic maps and conventional data were used to prepare the thematic layers of seven disease related parameters. The thematic layers and their corresponding features were assigned weights after deciding the relative importance of different themes in causing disease occurrence on a 1–9 scale, and the normalized weights were obtained using Saaty's AHP. Distribution of area in a district is represented in pie chart. It displays the information in an easy way. The bigger slice shows, the more of area occupied (Figure 13).

The above chart divides the study area into five JE potential zones, 'severe', 'high' and 'moderate', 'poor' , 'very poor' covering 27.19%, 28.29%, 33.08%, 6.99% and 4.61% of the study area, respectively. Since the major portion (more than 80%) of the study area exhibits moderate to severe disease potential area, it can be inferred that disease occurrence spread somewhat rapidly.

5 Validation of Disease Risk Zone Map

Validation of disease risk zone area with collected field JE disease death data block wise of year 2009 at locations is shown in Figure 13.

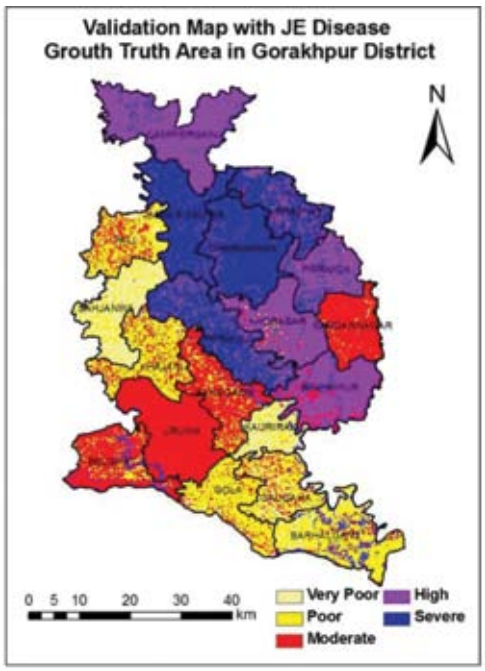

Figure 14: Validation Map of Disease Risk Zone Area

The areas in this risk zone map for severe, high, moderate, poor and very poor conditions are shown in Table 6.

Table 6 represents the comparative area with a predicted model and ground truth data of JE disease death of year 2009. The model is compared on the basis of different criteria, which include very poor, poor, moderate, high, and severe (with the range of number of JE disease cases). Less than 3 number of disease cases are predicted in 12.16 % range, while in ground truth it is 24.10 percent. About 4 to 6 number of cases lie in the 12.25% range of the predicted model, while at ground level it is 11.21 percent. Moderate number of, between 6 to 10, lie in the 12.87 % range of the predicted area and are at 23.43 percent for ground level. Very high and severe conditions of the disease are categorized in

the range of 10 to 13 and above 13, which is covers about 26.50 % and 24.07 % of the area model, although at ground level it is 12.87 % and 17.79 %.

Table 6: The comparative table from the predicted area and ground truth data

No.	Criteria	Ground truth data of Disease cases	Predicted area in Model (%)	The Ground Truth Area (%)
1.	Very Poor	< 20	21.16	24.10
2.	Poor	21-30	12.25	11.21
3.	Moderate	31-40	12.87	23.43
4.	Very high	41-50	26.50	24.07
5.	Severe	> 50	12.87	17.79

Table 6 represents the comparative area with a predicted model and ground truth data of JE disease death of year 2009. The model is compared on the basis of different criteria, which include very poor, poor, moderate, high, and severe (with the range of number of JE disease cases). Less than 3 number of disease cases are predicted in 12.16 % range, while in ground truth it is 24.10 percent. About 4 to 6 number of cases lie in the 12.25% range of the predicted model, while at ground level it is 11.21 percent. Moderate number of, between 6 to 10, lie in the 12.87 % range of the predicted area and are at 23.43 percent for ground level. Very high and severe conditions of the disease are categorized in the range of 10 to 13 and above 13, which is covers about 26.50 % and 24.07 % of the area model, although at ground level it is 12.87 % and 17.79 %.

This gives a realistic disease risk zone area map of the study area, which is used for health planning and development. Based on this result of study, concerned decision makers can formulate the model to justify that the moderate to high and high to moderate risk zone area occupy.

6. Conclusion:

In this study, Remote Sensing, GIS and multicriteria decision making techniques have been successfully used and demonstrated for evaluation of disease risk zone area. A three-step methodology was used that includes development of thematic layers, deriving the weights using AHP to find the risk block/zone. Remotely sensed satellite image data and digitization of existing maps using GIS were used for the preparation of thematic layers. The AHP were used to provide utility weights for the alternatives. In this study area, five categories of groundwater potential zone have been delineated based on remote sensing, GIS and AHP techniques.

Acknowledgement:

Author gratefully acknowledges the support and encouragement received from the Dr. R.D. Gupta, Professor, Department of Civil Engineering, Motilal Nehru National Institute of Technology, Allahabad, of this research work and is thankful to Dr. K. N. Pandey, D.M.O. Gorakhpur for collection of disease information and suggestions.

References:

1. Albayrak Esra (2004). Using analytical hierarchy process (AHP) to improve human performance: An application of multiple criteria decision making problem. Journal of Intelligent Manufacturing 15, 491-503, 2004.

2. Balasubramanian A., Tyagi B.K., (2009). Sero-entomological investigations on Japanese fencephalitis outbreak in Gorakhpur division, Uttar Pradesh, India. Indian J Med Res 129, March 2009, pp 329-332.

3. Fischer Marc, Lindsey Nicole, Staples Erin J., (2010). Morbidity and Mortality Weekly Report. Recommendations and Reports. Vol. 59 / No. RR-1.

4. Jankowski, P., 1995, Integrating geographical information systems and multiple criteria decision making methods.International Journal of Geographical Information Systems, 9, pp. 251–273.

5. JUN, C., 2000, Design of an intelligent geographic information system for multi-criteria site analysis.URISA Journal, 12, pp. 5–17.

6. Liu Xue-Hua, Skidmore K. A., Oosten Van. H., (2002). Integration of classification methods for improvement of land-cover map accuracy. ISPRS Journal of Photogrammetry & Remote Sensing 56:257–268.

7. Malczewski, J., 1996, A GIS-based approach to multiple criteria group decision-

making. International Journal of Geographical Information Systems, 10, pp. 955–971.

8. Malczewski, J., 1999, GIS and Multicriteria Decision Analysis(New York: Wiley).

9. Malczewski, J., 2000, On the use of weighted linear combination method in GIS: common and best practice approaches.Transactions in GIS, 4, pp. 5–22.

10. Murray C. J. L., Shengelia B., Gupta N., Moussavi S., Tanjon A., Thieren M. (2003). Validity of Reported Vaccination Coverage in 45 Countries. Lancet. 362(9389):1022–27.

11. Raban Z Magdalena, Dandona Rakhi, Dandona Lalit (2009). Essential health information available for India in the public domain on the internet. BMC Public Health2009, 9:208.

12. Solomon Tom, Dung Minh Nguyen, Kneen Rachel, Gainsborough Mary, Vaughn W David, Khanh Thi Vo (2000). Japanese encephalitis, J Neurol Neurosurg Psychiatry2000, 68:405–415.

13. Parida M. M., Santhosh R S.., Dash K. P, N. K. Tripathi, Saxena P., Ambuj S., Sahni K. A., Rao V. P. Lakshmana, Kouichi Morita (2006). Development and Evaluation of Reverse Transcription–Loop-Mediated Isothermal Amplification Assay for Rapid and Real-Time Detection of Japanese Encephalitis Virus. Journal Of Clinical Microbiology, Nov. 2006, p. 4172–4178.

14. Saxena Shailendra K., Mishra Niraj., Saxena Rakhi., Singh Maneesh., Mathur Asha., (2009). Trend of Japanese encephalitis in North India: evidence from thirty-eight acute encephalitis cases and appraisal of niceties. J Infect Dev Ctries 2009; 3(7):517-530.

15. Sabesan Shanmugavelu , Raju Konuganti Hari Kishan, Perumal Vanamail (2008). Spatial Delimitation, Forecasting and Control of Japanese Encephalitis: India – A Case Study. The Open Parasitology Journal,2008, 2, 59-63.

16. Saxena K. Shailendra., Tiwari Sneham., Saxena Rakhi., Mathur Asha., P.N. Nair Madhavan., (2008). Japanese Encephalitis: An Emerging and Spreading Arbovirosis. In: Růžek D, editor. Flavivirus Encephalitis. Rijeka, Croatia: InTech. pp. 295–316.

17. Saaty R.W., (1987). The Analytic Hierarchy Process – What it is and How it is used. Mathi Modelling, Vol. 9, No. 3-5, pp, 161-176.

18. Saaty L. Thomas., (1996). Decision Making with Dependence and Feedback: The Analytic Network Process. RWS Publications, 1996, ISBN 0-9620317-9-8.

19. Saaty L. Thomas., (2004). Fundamentals Of The Analytic Network Process-Multiple Networks With Benefits, Costs, Opportunities And Risks. JOURNAL OF SYSTEMS SCIENCE AND SYSTEMS ENGINEERING Vol. 13, No. 3, pp348-379, September, 2004.

20. Singh Arvind., (2007). Menace of Japanese encephalitis inrural areas of eastern Uttar Pradesh. Current Science, Vol. 93, No. 12, 25 December 2007.

21. Srivastava V.K., Ajay Singh., Thapar B.R., (2008). Field evaluation of malathion fogging against Japanese encephalitis vector, Culex tritaeniorhynchus. J Vector Borne Dis45, September 2008, pp. 249–250.

22. World Health Organization. WHO position statement on integrated vector management Weekly Epidemiol Rec. 2008;83:177–81.

3D City Modelling

Marica Franzini, Vittorio Casella, Geomatics Laboratory, Department of Civil Engeeniring and Architecture, University of Pavia, Italy

1. The University of Pavia

Pavia is a Municipality located in north-west Italy, 35 kilometres far from Milan, with a population of about 68.000 inhabitants.

The University of Pavia, one of the most ancient universities in Europe, was founded in 1361; it offers several bachelor, master and PhD courses in a wide range of academic areas among which the Engineering (official website: http://www.unipv.eu/site/en/home.html).

The Geomatics Laboratory belongs to the Department of Civil Engineering and Architecture and it is devoted to researches on surveying and mapping topics such as topography and GNSS technologies, aerial and UAS photogrammetry, lidar, digital cartography and GIS. The Laboratory gives support to teaching activities within three courses: "Topography" and "Theory and practice of GPS surveying" for the bachelor degrees and "Photogrammetry, Lidar and GIS" for the master ones.

2. Photogrammetry, Lidar and GIS Course

The course is addressed to the students of the two Master Degrees in Civil Engineering and Environmental Engineering. It is subdivided in two parts: during the first one, the lectures are mainly theoretical and students learn about surveying techniques (such as aerial photogrammetry and lidar), cartographic products (digital maps, orthophotos, digital models) and GIS. Instead, the second part of the course is largely devoted to practical activities in order to apply some of the concepts learnt before.

The students are usually involved in photogrammetric projects for the purpose of realizing 3D models of different areas of the Pavia's city. Up to this year, when PHOTOMOD Lite was introduced, the students performed the photogrammetric workflow using different software, sometimes homemade (some tools were written in Matlab); PHOTOMOD Lite has allowed to complete the whole process, from inner orientation to stereo-plotting, into one single environment improving the teaching quality.

The program was installed at the Department's informatics classroom (Figure 1) on 56 PC where 61 students were involved in the course activities, during the last academic year (2015/2016).

Figure 1. Department's informatics classroom

3. Course's Project

The former military depot of Pavia is a large area located in the west part of the city near the Ticino river (Figure 2). The depot is now decommissioned by the Ministry of Defence and it is into a state of neglect.

The main historical part was built between 1861 and the first half of the '900. Inside the area, there are several buildings different by size, age of construction, type and state of conservation as warehouses, in line buildings and production specialist buildings, also of recent times; its surface is characterized by large green areas crossed by paved paths and squares. The area is crossed from north to south by a little water channel, the Navigliaccio, which divides the area almost in half (Figure 3). The entire complex has an area of about 140,000 square meters.

Figure 2. The dismissed military depot area highlighted on the orthophoto of Pavia

In 2014, by the Decree of the Ministry of Economy and Finance, the area was declared no longer useful for the institutional purposes of the Department of Defence and returned to Pavia's Municipality. Now, the area is object of restoration projects.

Figure 3. Orthophoto of the dismissed military depot

4. Data description

Pavia has a long photogrammetric tradition. In the last two decades, it was involved, as a test site, in several projects on direct photogrammetry and on the use of native digital camera (1st and 2nd generation of AD40 cameras).

In 2003, Pavia was leader of a national project on the use of GPS/IMU sensor for direct photogrammetry where several blocks were acquired in different configurations (by focal lengths, flying heights, block structures) and more than 200 GCPs (Ground Control Points) were created and measured as a support for aerial triangulations.

A little part of this dataset was used within PHOTOMOD software during the course.

For educational purposes, one single strip, composed by three images, forms the aerial block (Figure 4). The images were acquired in May 2003 by the Italian company CGR whose plane is equipped with a 150 mm Leica RC30 camera. The flying height was 750 m so the GSD (Ground Sampling Distance) was approximately 7 cm. The original film support was scanned with a pixel resolution of 14 microns (namely 1800 dpi resolution). Table 1 shows the main camera parameters contained inside the calibration certificate.

Figur e 4. Block structure

General information

Camera Type	RC30
Lens Type	15/4 UAG -S
Calibration date	14.12.2001

Principal characteristics

Focal length [mm]	153.314	
PPA (principal point of auto -collimation) [mm]	-0.005	-0.001
PPS (principal point of symmetry) [mm]	-0.004	-0.009

Fiducial marks

	x [mm]	y [mm]		x [mm]	y [mm]
1	106.001	-106.000	5	-0.002	-111.996
2	-106.001	-105.999	6	-112.001	0.000
3	-106.001	106.000	7	-0.001	112.000
4	106.003	106.001	8	112.003	0.002

Radial distortion

Radius [mm]	Mean radial distortion [µm]	Radius [mm]	Mean radial distortion [µm]
10	-0.6	90	-0.2
20	-1.2	100	0.5
30	-1.4	110	1.1
40	-1.3	120	1.3
50	-1.3	130	0.8
60	-1.2	140	0.1
70	-1.1	148	-1.1
80	-0.7		

Table 1. Camera parameters

Pavia's Test Site has many relevant features which have been developed since 1999, according to the needs of the ongoing researches on photogrammetry. Among these features there are more than 200 artificial GCPs constituted by white squares of 35 cm directly painted on roads or other flat concrete structures.

The GCPs were measured with GPS in the fast-static mode, using three fixed receivers, set up on vertices of a GPS network, forming an equilateral triangle. The relative redundancy of the adjustment was therefore three, and results were very good, as Table 2 shows.

	min [cm]	max [cm]	mean [cm]	std [cm]
e	0.16	0.80	0.44	0.34
n	0.16	0.73	0.31	0.01
h	0.33	1.50	0.90	0.25

Table 2. Mean statistical parameters of GCPs

5. Project workflow

In this section, it will be described the main steps followed to perform photogrammetric workflow. To each student, it has been requested to follow these stages:

1. Creation of PHOTOMOD project
2. Importing of imagery and GCPs
3. Inner orientation
4. TP generation
5. GCPs collimation
6. Bundle adjustment

The aim of each section was to explain, with practical activities, the theory explored during the first part of the course; the students can better understand the meaning of each procedure with direct experience (difference between ground and tie points, interior and exterior orientation, etc.).

Each step was explained by the teacher and showed to the classroom; with the support of several Italian lecture notes (especially prepared), each student was able to elaborate autonomously each stage and verify the obtained results.

5.1. Project creation and data importing

The photogrammetric block used a projected system – WGS84 UTM32N – and is composed by three frames forming a single East-West strip. The imagery was imported and the pyramids were calculated (Figure 5).

The ground truth was composed by 9 artificial GCPs constituted by white square directly painted on the ground. In Figure 6 is shown a portion of a monography and an example of GCP. The final distribution of the whole set of GCPs is shown in Figure 7. It is noticeable that no cartographic information is available in the area of interest (highlighted with a red square) due to its original military purpose.

Finally, Figure 8 shows the result of the GCPs importing: the cartographic coordinates (East, North and Up components) and the standard deviations used for bundle adjustment (1 cm for planimetric components and 1.5 cm for altimetric one).

Each student has evaluated the results of this preliminary step, through a simple visual inspection of the graphic interface of PHOTOMOD Lite software.

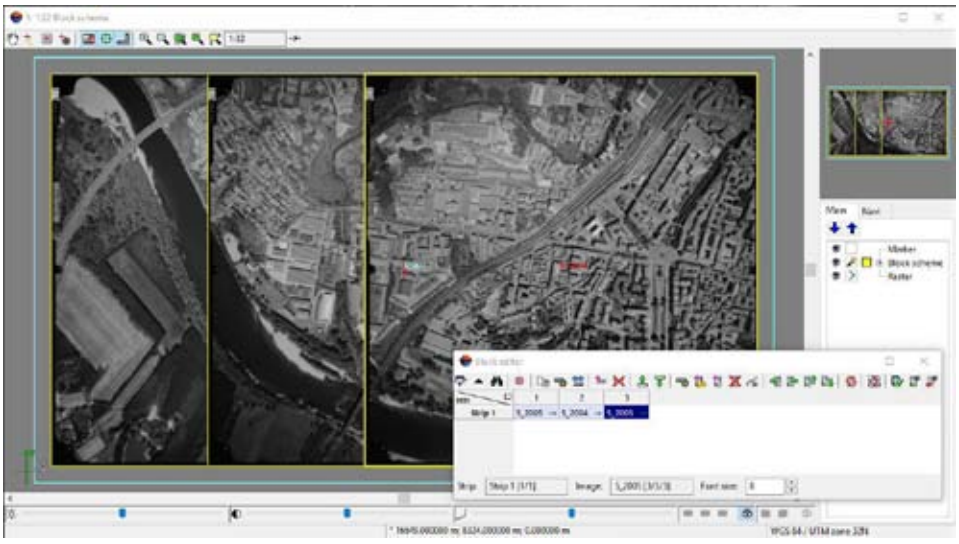

Figure 5. The result of the imagery importing

Figure 6. Example of GCP: on the left is shown a portion of the original monography and on the right an image taken on the ground

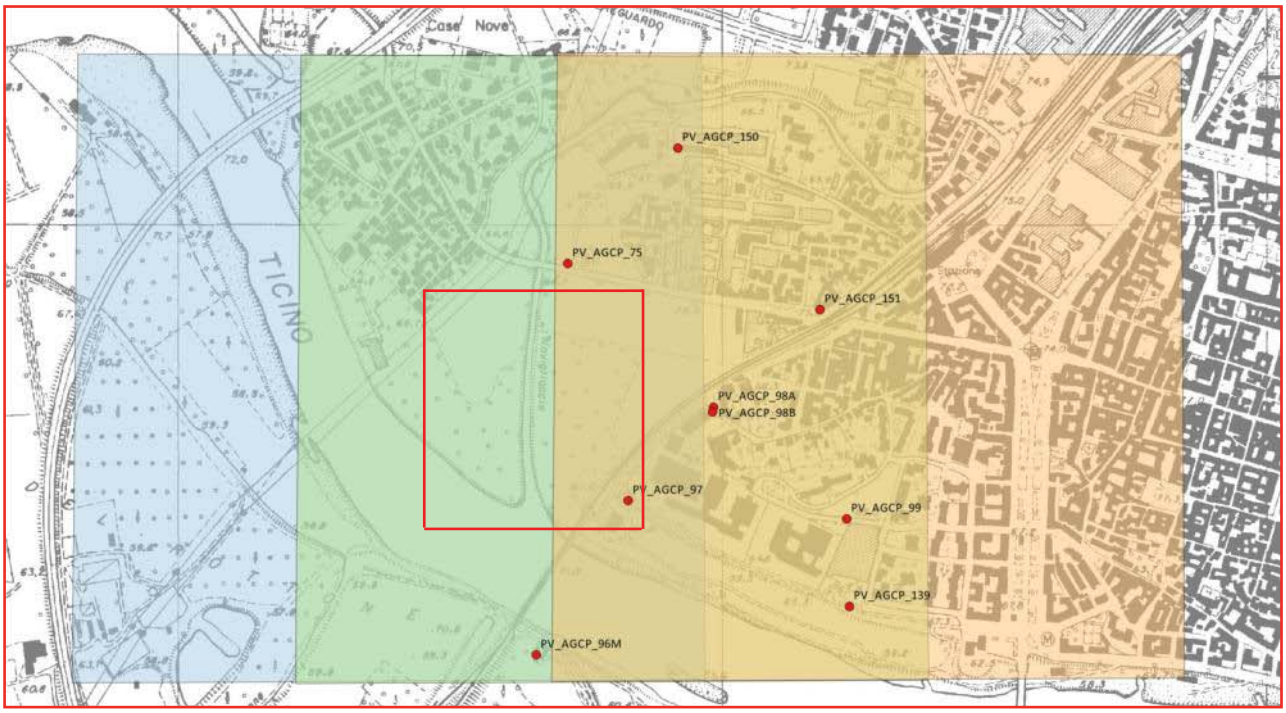

Figure 7. The distribution of the 9 GCPs and the position on the project area

Import Ground Control Points

Name	X, m	Y, m	Z, m	Std. dev. X,...	Std. dev. Y,...	Std. dev. Z,...
PV_AGCP_150	510890.079	5004121.301	110.116	0.01	0.01	0.015
PV_AGCP_151	511151.637	5003824.304	110.43	0.01	0.01	0.015
PV_AGCP_74	510611.358	5004309.544	108.997	0.01	0.01	0.015
PV_AGCP_75	510688.025	5003908.567	106.544	0.01	0.01	0.015
PV_AGCP_96M	510629.687	5003189.293	101.255	0.01	0.01	0.015
PV_AGCP_97	510799.111	5003472.688	106.102	0.01	0.01	0.015
PV_AGCP_98A	510955.878	5003645.064	108.8	0.01	0.01	0.015
PV_AGCP_98B	510953.657	5003635.718	108.27	0.01	0.01	0.015
PV_AGCP_99	511200.625	5003439.291	106.856	0.01	0.01	0.015

OK Cancel

Figure 8. The result of the GCPs importing

5.2. Interior orientation

The camera management tool was used to create a new calibration certificate; the information about the camera was given to each student (see also Table 1).

For the didactics purposes of the project, all the images were manually oriented (Figure 9). The students can evaluate their inner orientation through the use of the partial and final reports proposed by the software (Figure 10); if the results exceeded the fixed threshold (0.01 mm) they must repeat the orientation otherwise they can proceed to the next step.

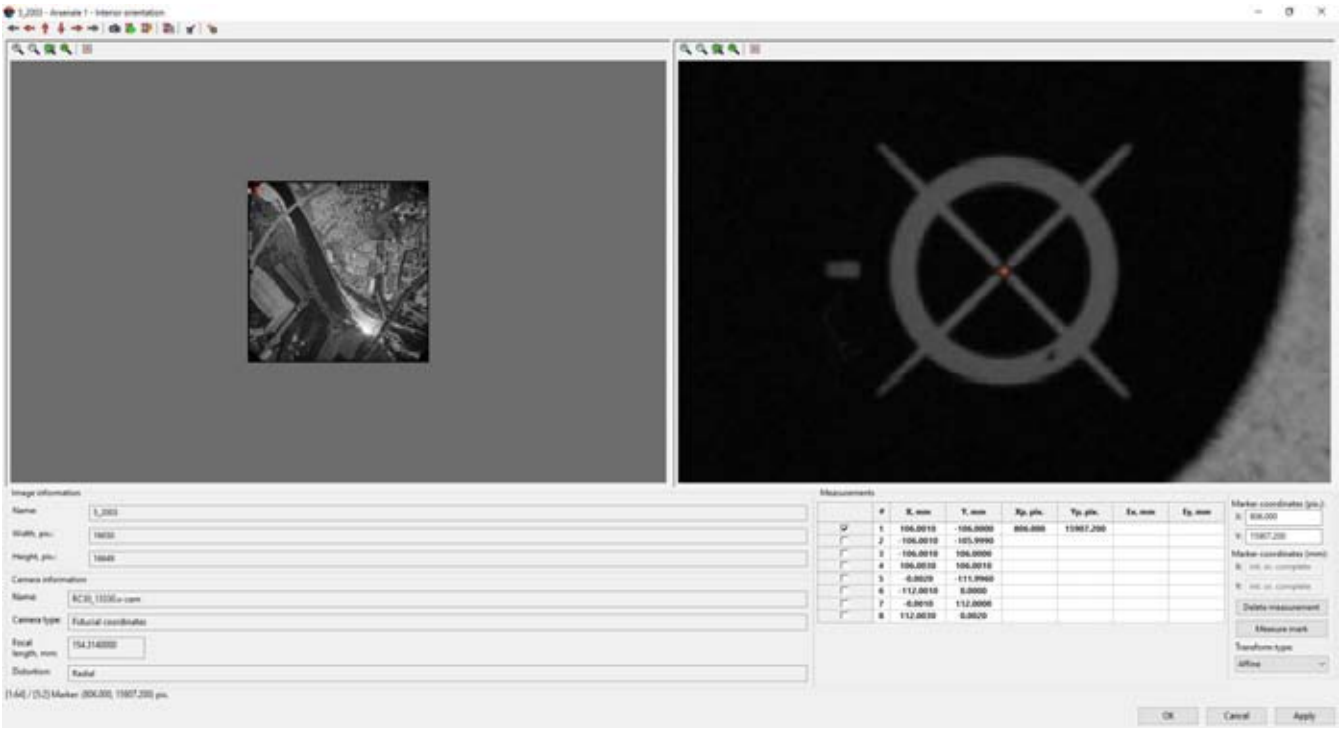

Figure 9. Manual interior orientation interface

Strip: Strip 1

	Image	Camera	Camera type	Axes orientation	Number of fiducials measured	Transform type	Residuals, RMS, mm
*	5_2003	RC30_13330.x-cam	Fiducial coordinates	180°	8/8	Affine	0.0084
*	5_2004	RC30_13330.x-cam	Fiducial coordinates	180°	8/8	Affine	0.0066
*	5_2005	RC30_13330.x-cam	Fiducial coordinates	180°	8/8	Affine	0.0056

Figure 10. The results of the interior orientation: the final residuals are under the fixed threshold of 0.01 mm

5.3. TP generation

The Tie Points (TPs) measurements were performed automatically through the dedicated tool in which the strategies for their extraction were fixed (numbers, correlation threshold, strategy for transferring, etc.). Also for this step, the students were able to evaluate the results of the procedure visually inspecting the TPs extracted (Figure 11) and analysing the Relative Orientation Report (Figure 12).

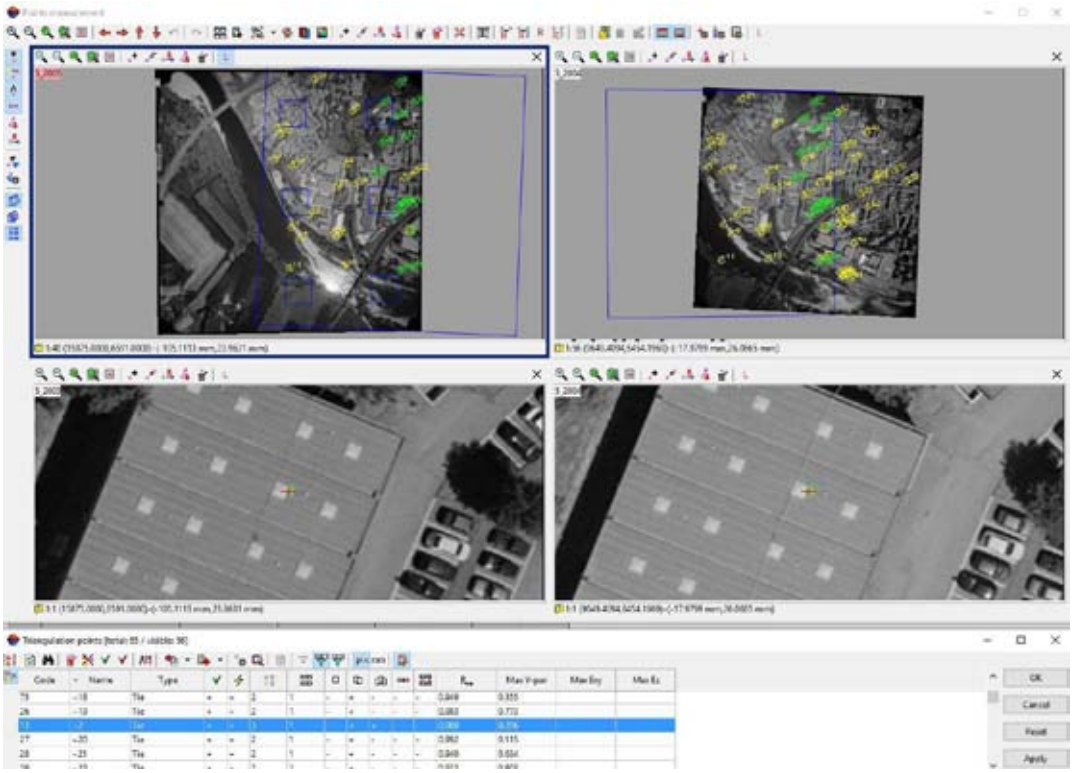

Figure 11. Examples of the TPs automatically extracted by the software

Strip: Strip 1

	Stereopair	Number of points	Vertical parallax, pix.			Discrepancy of kappa angle, rad	Distribution uniformity	
			RMS	Mean abs.	Max			
*	5_2003—5_2004	33	0.470	0.384	0.959	-0.00766362	Non-uniform	+ –
*	5_2004—5_2005	38	0.283	0.223	0.931	0.01201098	Non-uniform	+ –

	Triplet	Number of points	Tie residuals, pix.					
			RMS		Mean abs.		Max	
			E_{xy}	E_z	E_{xy}	E_z	E_{xy}	E_z
*	5_2003—5_2004—5_2005	15	0.391	0.678	0.331	0.606	0.679	1.075

Figure 12. The Relative Orientation Report

5.4. GCPs collimation

All the GCPs were measured manually by the students using the Points Measurement tool (Figure 13a) and the monography distributed. Each GCP was measured in each frame in which it was visible; some GCPs are visible in three images while the others only in two.

Besides, three GCPs were used for check control after bundle adjustments so they were labelled as "Check" in the Triangulation Points window (Figure 13 b). 5.5. Bundle adjustment

Bundle adjustment was performed using all

a)

Triangulation points [total: 64 / visible: 8]

GCP list | All triangulation points

Point properties

Code	Name	Type	X, m		m
78	PV_AGCP_139	Ground Control	511205.408	5003278.543	107.573
65	PV_AGCP_150	Check	510890.079	5004121.301	110.116
66	PV_AGCP_151	Ground Control	511151.637	5003824.304	110.43
68	PV_AGCP_75	Ground Control	510688.025	5003908.567	106.544
69	PV_AGCP_96M	Ground Control	510629.687	5003189.293	101.255
70	PV_AGCP_97	Check	510799.111	5003472.688	106.102
72	PV_AGCP_98B	Ground Control	510953.657	5003635.718	108.27
73	PV_AGCP_99	Check	511200.625	5003439.291	106.856

b)

Figure 13. (a) Un example of the visibility of the artificial GCP on an image; (b) the selection of the typology of points: Ground Control or Check Points

the data introduced into the software – Tie Points and Ground Control Points image coordinates and GCPs ground ones. The weight of GCPs was set as reported in section 5.1 (1 cm for planimetric components and 1.5 cm for altimetric one). The point on image measurement precision was set equal to ½ pixel for manual measurement and 1 pixel for automatic one.

In this step, the student can evaluate their aerial triangulation analysing the block adjustment report with particular attention on the ground control and check points residuals (Figure 14). Since the GSD was 7 cm, the final results were less than ½ GSD for planimetric coordinates and less than 1 GSD for altimetry.

Ground control point residuals

N	Xm-Xg	Ym-Yg	Zm-Zg	Exy (metre)
PV_AGCP_139	0.001	0.001	0.001	0.002
PV_AGCP_151	-0.002	-0.002	-0.003	0.003
PV_AGCP_75	-0.000	0.004	0.001	0.004
PV_AGCP_96M	0.001	0.000	-0.001	0.001
PV_AGCP_98B	0.000	-0.003	0.002	0.003
mean absolute:	0.001	0.002	0.002	0.003
RMS:	0.001	0.003	0.002	0.003
maximum:	0.002	0.004	0.003	0.004

Check points residuals

N	Xm-Xg	Ym-Yg	Zm-Zg	Exy (metre)
PV_AGCP_150	0.037	0.012	-0.045	0.039
PV_AGCP_97	0.011	-0.001	0.049	0.011
PV_AGCP_99	0.017	0.013	0.016	0.021
mean absolute:	0.022	0.009	0.037	0.024
RMS:	0.024	0.010	0.026	0.026
maximum:	0.037	0.013	0.049	0.039

Figure 14. A part of the block adjustment report where residuals on GCPs and CPs were reported

The possibility to set some marker as CPs allows to better understand how interpret the results of a bundle adjustments, in particular the difference between the residuals on GCPs and CPs. The final report was also useful to understand the others results of aerial triangulation as the exterior orientation parameters of each frame and ground coordinates of tie points.

6. 3D modelling

The final step of the project was the stereo-plotting of the Arsenale' area.

The students were subdivided into 18 groups and to each groups was assigned a cluster of buildings. The Laboratory gave to each student a pair of anaglyph glasses in order to perform stereo restitution.

Each group has requested to:

- Create a set of vector layers (one for each building)
- Open the stereo-pair window in anaglyph mode
- Activate the stereo vision
- Draw the roof of each building with a closed polyline (Figure 15)

Even if some building have roofs with strange and complicate structures, the tool Roof was successfully used in many cases for the simple ones.

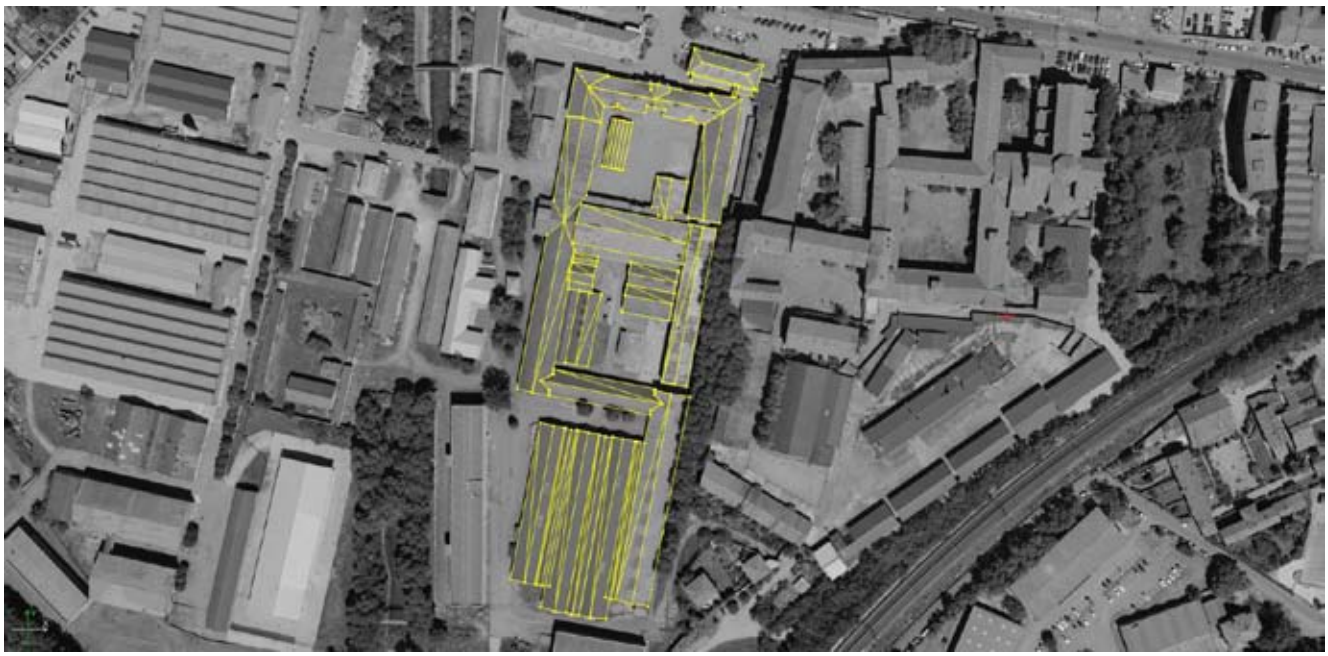

Figure 15. Example of the stereo-plotted roofs

Finally, the 3D-Mod module was used to reconstruct the 3D model of the stereo-plotted buildings. Figure 16 shows an example of the model build for oldest part of the project area and Figure 17 a particular of this complex building.

The 3D model of each building was then exported in dxf format and imported in Trimble Sketchup where imagery acquired on the ground was applied as texture. Some views of the final product are shown in Figure 18.

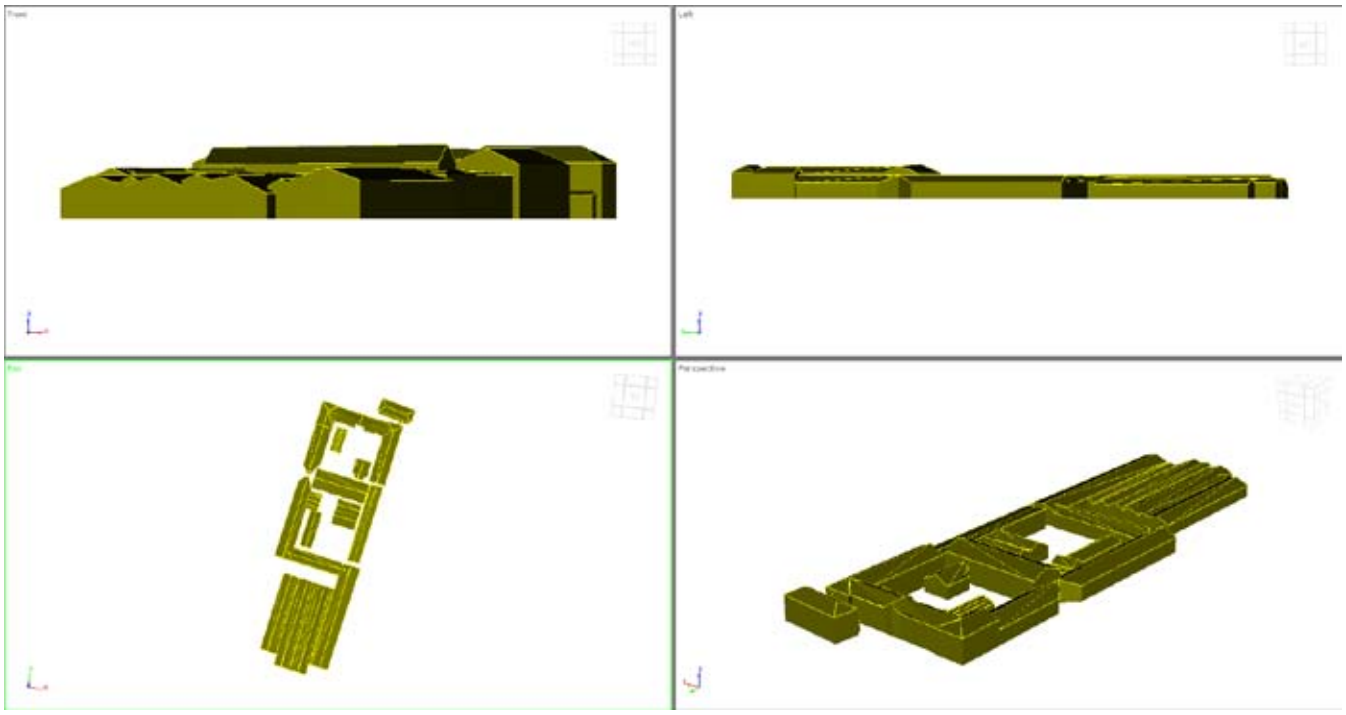

Figure 16. The 3D model reconstructed inside 3D-Mod

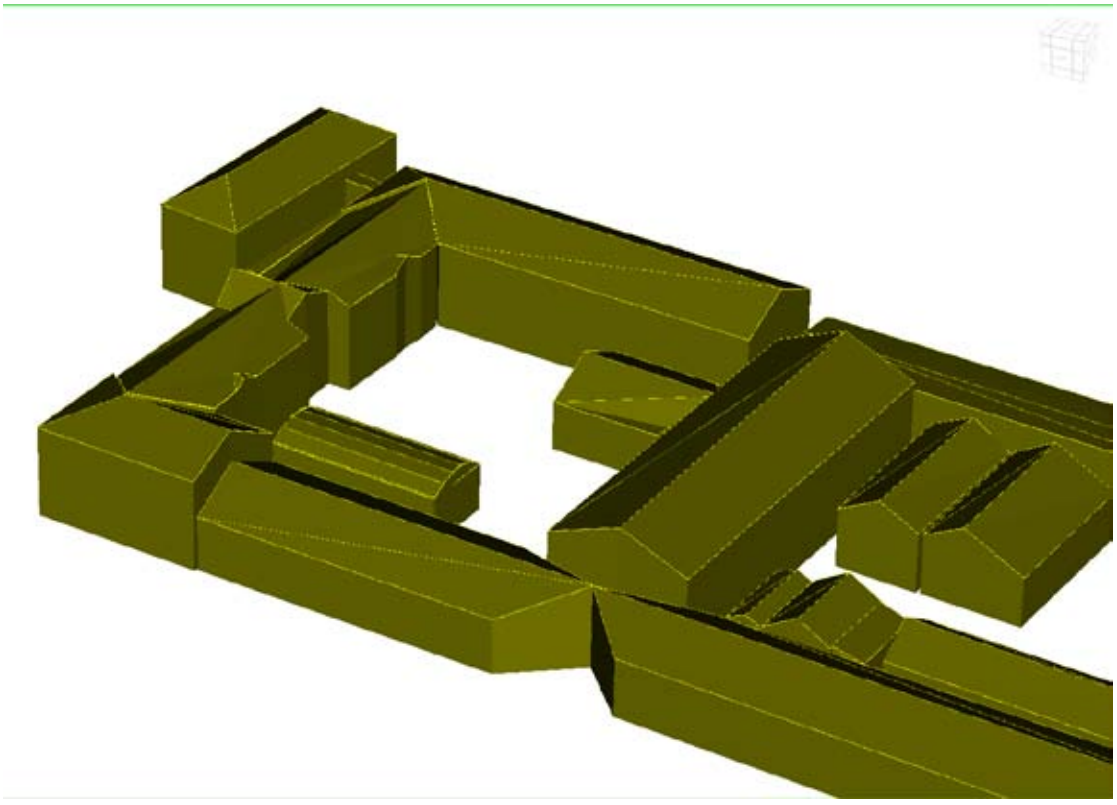

Figure 17. A particular of the 3D model reconstructed inside 3D-Mod

Figure 18. Some views of the final 3D model with photorealistic textures

New choice of 50 cm satellite imagery

Wook-Hyun Choi, SI Imaging Services, Korea

SI Imaging Services (SIIS) started commercial services of KOMPSAT-3A imagery with the world's second highest resolution satellite from July, 5th. KOMPSAT-3A is part of the Korean Multipurpose Satellite Program developed and operated by the Korea Aerospace Research Institute (KARI) for earth observation purpose. The earth observation satellite offers clear imagery with a resolution less than 0.5 meter. KOMPSAT-3A, also known as Arirang-3A, was launched into orbit in March last year. After more than a year of successful test operation, SIIS began the commercial services on 5th of July. It would make South Korea the world's second country to enter the less-than-0.5-meter-resolution satellite imagery market after the United States.

KOMPSAT-3A is the sister of KOMPSAT-3, using the same satellite bus and payload. Its local access time is very unique in the afternoon, 13:30, which is the same with KOMPSAT-3. However, since KOMPSAT-3A was put into lower orbit than KOMPSAT-3, it delivers clearer and sharper view. The same imaging time and similar payload with KOMPSAT-3 will amplify its capacity and help to even out the difference of the color. With KOMPSAT-3A imagery available today with 0.5 meter resolution imagery of KOMPSAT-3 at customer's service, decision makers have new and more options to consider for their needs.

PHOTOMOD 6.2. New functionality

Dmitry Kochergin, Racurs, Russia

The most interesting new features of PHOTOMOD 6.2 are the new interface of PHOTOMOD UAS software and new reliable feature-based algorithm of tie point measurements over UAS imagery.

Besides Dense DSM (SGM method) now works with a subpixel accuracy and one of the output products of this process is a point cloud in LAS format "colored" by using pixels of source images, which makes a model more realistic.

Last supported satellite sensor models are VNREDSat-1, DubaiSat-2 and KompSat-3. GDAL library is used to import more raster and vector formats.

Also we have added some improvements to dodging color balancing process and cut-and-fill analysis.

Estimation of KOMPSAT-3 Imagery Potential for DSM Creation

Anatoly Zubarev, Aleksandr Chekurin, Racurs, Russia

The present research was a stage of the complex project on KOMPSAT-3 stereo images testing conducted by specialists of Racurs company in DPW PHOTOMOD.

Introduction

Presently, satellite stereo survey becomes more and more popular. Many new RSD satellites will be launched in the next years and dozens are successfully operated today. Racurs's team has tested KOMPSAT-3 stereopair (GSD = 0.8 m, convergence angle = 44 degrees) and evaluated accuracy of KOMPSAT-3 digital surface model (DSM) vs DSM from aerial survey (GSD = 0.18 m).

The following characteristics of KOMPSAT-3 data were tested:

- RPC accuracy;
- Stereopair inner geometry;
- Stereopair DSM accuracy comparing with aerial survey DSM.

The estimation of RPC accuracy and internal geometry of stereopair

10 well-recognizable terrain objects (building and fence corners, road intersections) were used as the ground control points (GCP) in the test. The coordinates of GCPs were measured on the images of the high accuracy aerial survey project.

The adjustment of KOMPSAT-3 stereopair with using no GCPs (bias method) gives the estimation of the source RPC coefficients (RMSxy = 18.1 m and RMSz = 0.65 m). Usage of only one GCP allows to compensate systematic RPC errors. The final adjustment errors on check points for this experiment are: RMSxy = 0.8 m and RMSz = 0.65 m. In the experiment with all GCPs included into the adjustment RMSxy = 0.42 and RMSz = 0.42 m (on control points).

Output DSM quality estimation

In order to estimate the accuracy of DSM built by KOMPSAT-3 stereopair we used the reference DSM for the same area computed by the aerial survey project mentioned above (UltraCam camera). “Aerial” DSM has the cell size = 0.18 m while the “satellite” DSM cell size is equal to 0.7 m. Both DSMs were built by using the same SGM algorithm in PHOTOMOD 6.02 to make the experiment more objective.

Fig.1 shows DSM from KOMPSAT-3, Fig. 2 represents DSM calculated from the aerial imagery.

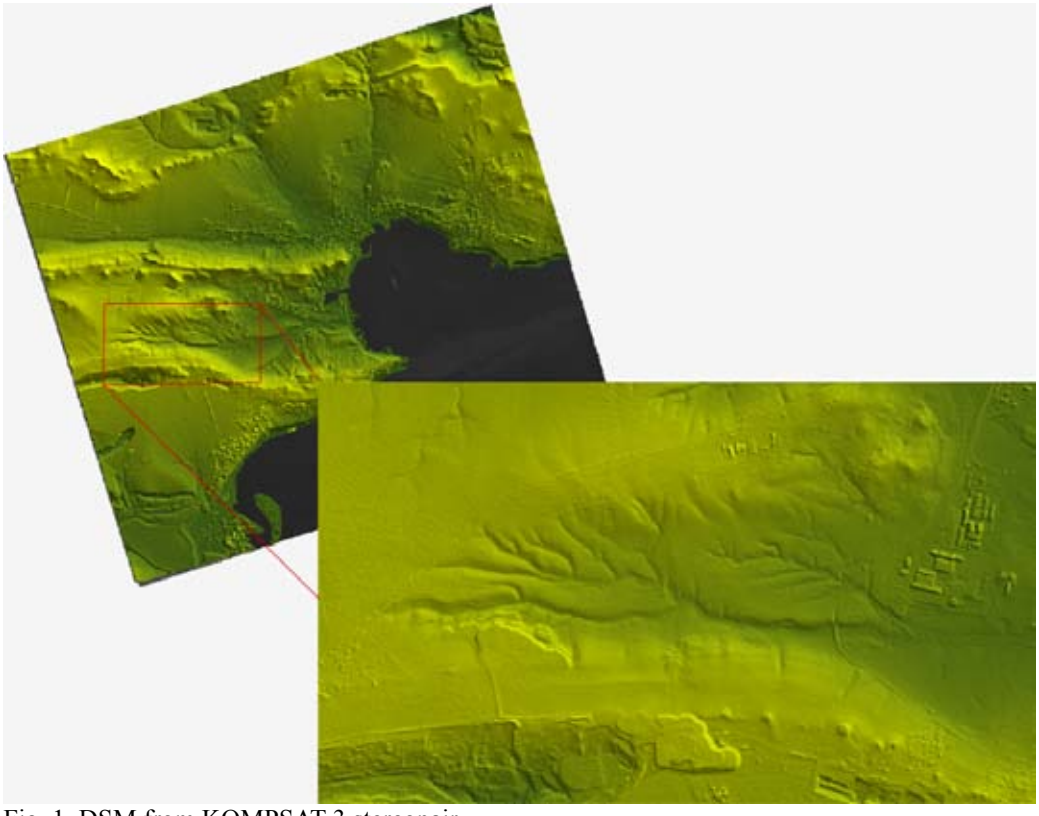

Fig. 1. DSM from KOMPSAT-3 stereopair.

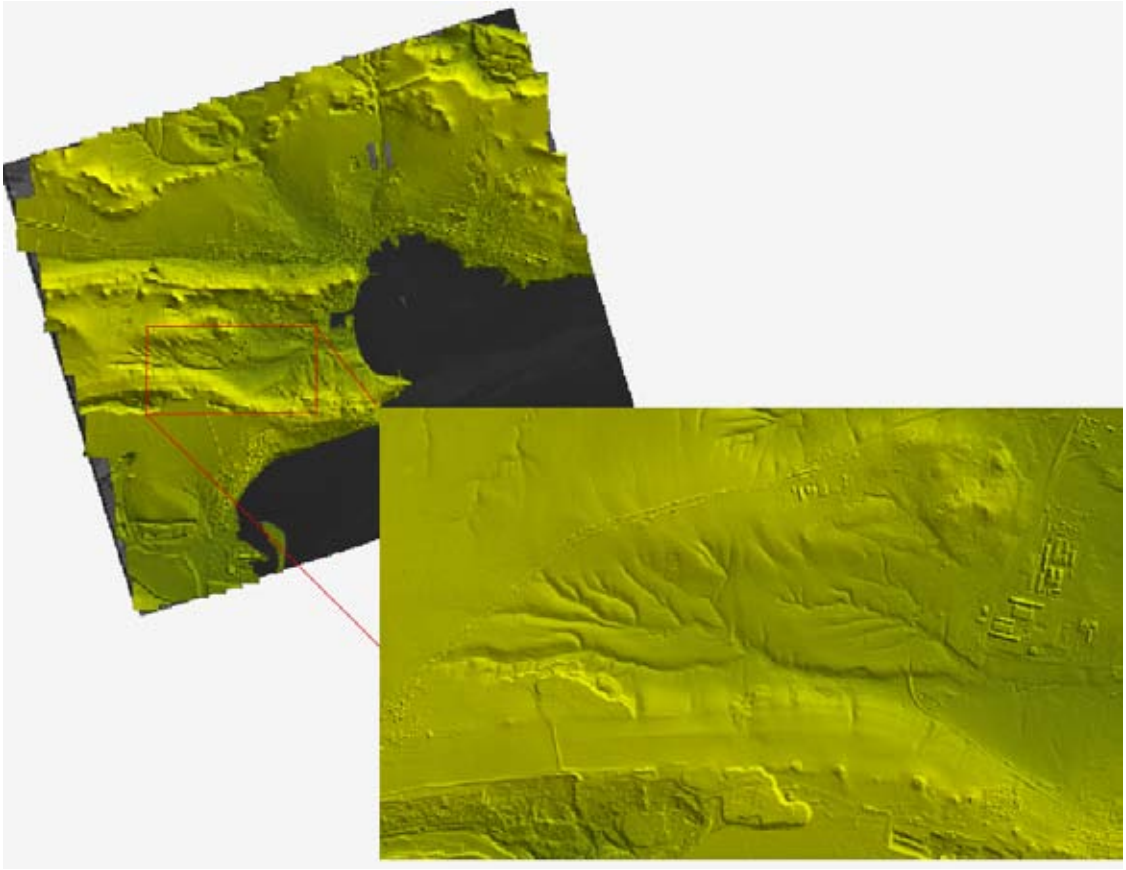

Fig. 2. DSM from the aerial survey

Calculation of histogram illustrated on Fig.3 was based on the Difference DEM. The Difference DEM was computed by dividing "aerial" DSM from "satellite" DSM.

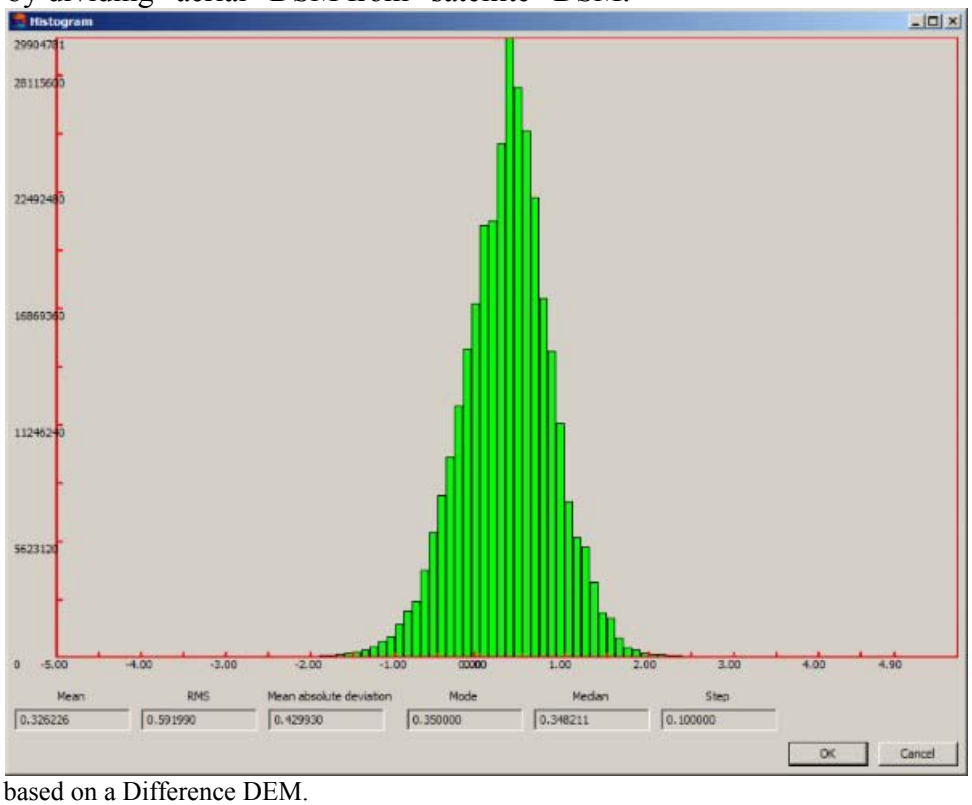

Fig. 3 Histogram based on a Difference DEM.

During the accuracy estimation the area was divided into three types according the following categories:

1. area with rivers and low degree of vegetation coverage,
2. rough terrain area with quarries, ravines,
3. urban area with city infrastructure (buildings, bridges, etc).

Taking into account these 3 categories histograms of Difference DEMs were created. Histograms are presented on Fig. 4 – Fig. 6.

After analyzing these histograms we can make the following conclusions:

1. Systematic DSM errors (both XY and Z) are very minimal (not greater than 0.2-0.4 m) that corresponds the adjustment accuracy and makes the further analysis possible;
2. All histograms have normal distribution shape typical for the case of random errors only;
3. Histograms from Fig. 4 – 6 look very similar but the histogram of the category 2 has more values over 2 meters in comparison with the histogram of the category 1. The main reasons of some inaccuracy in detecting edges of quarries are the big convergence angle and small number of images in the project (only two). As a result we have many blind areas over the stereopair;
4. Histogram 3 (Fig. 6) has maximim number of relevant exceeding 2 meters since the urban area has the biggest number of blind fragments.

These results of experiments enable to consider KOMPSAT-3 stereo images as a data with high geometrical quality. Vertical accuracy is differing in accordance with the area type:

RMSE = 0.46 m for area with rivers and low degree of vegetation coverage;

RMSE = 0.67 m for rough terrain area with quarries and ravines;

RMSE = 2 m for urban area with city infrastructure (buildings, bridges, etc).

Thus, RMSE for all plot area equals 0.6 m.

High vertical accuracy for this data is a result of geometrical quality and an optimal intersection angle = 44 degreases.

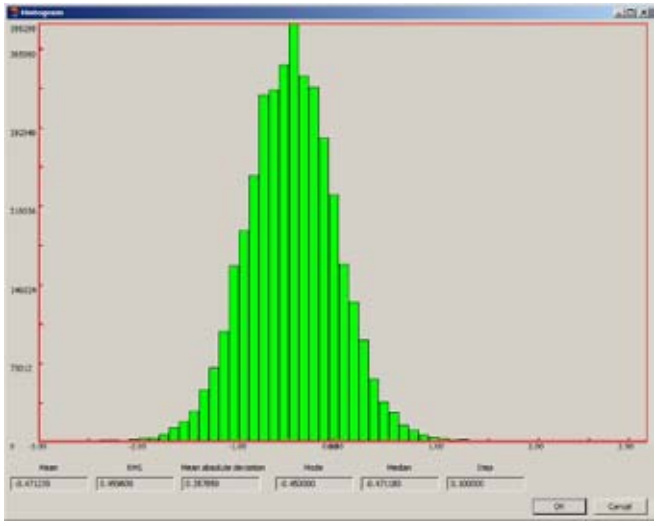

Fig. 4 Difference DEM for the Category 1

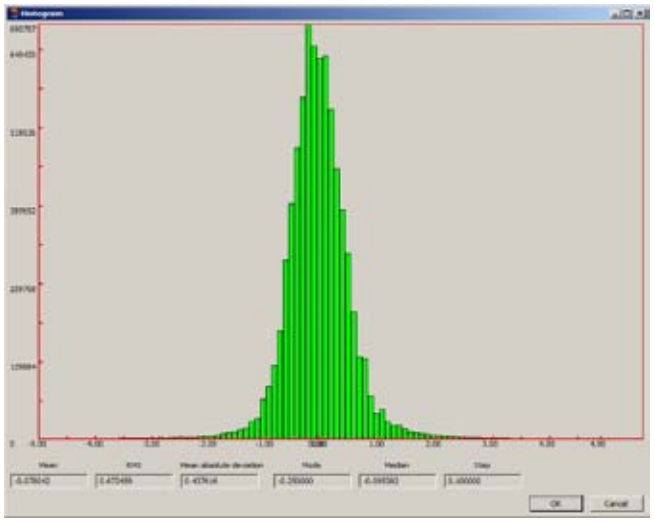

Fig. 5 Difference DEM for the Category 2

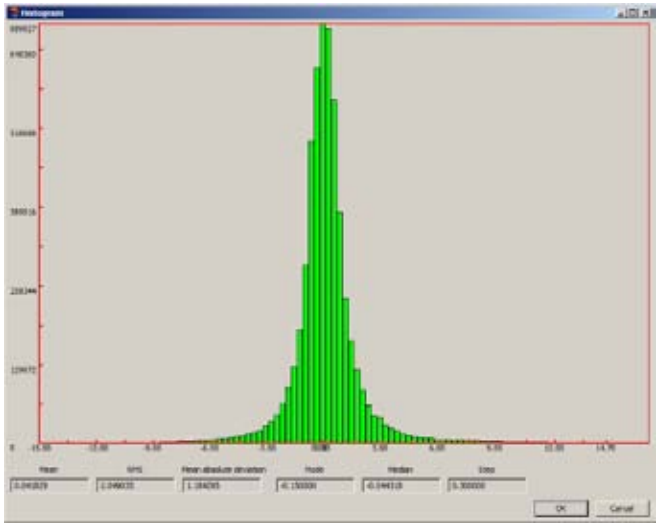

Fig. 6 Difference DEM for the Category 3

Kanopus-V: user experience and future development

Victor Nekrasov, VNIIEM Corporation, Russia

In this article was held the analysis of areas, in which can be used Kanopus-V data. Author done the assessment of tasks, which use Kanopus-V data. There was selected area for the use of data for mapping. The analysis of data quality from the point of view of their use for cartographic purposes, for creating and updating maps of scale 1:25000, which implies the required accuracy for the geolocation data. It is shown that the accuracy of the geolocation, using orbital data does not fully meet the requirements for creating maps, so you need to use the reference raster information database. The article describes a prospective satellite constellation of the Kanopus-V, which will be created in accordance with the Federal Space Program.

Comparison of point clouds produced by the technology ALS and DAP with automatic photogrammetric clouds

Aleksandr Voitenko, Kadasrtsurvey, Russia

Aerial lidar scanning and digital aerial photography (ALS and DAP) have been in the geoinformation services market for years now, and their accuracy parameters have been confirmed on numerous occasions. ALS and DAP enable to obtain digital orthophotomaps (DOPM), digital area/terrain models (DAM/DTM), 3D area models, and to create digital topographic layouts in various scales on their basis.

The technology of automatic photogrammetric processing of digital images (acquisition of a cloud of points based on digital images) is gaining popularity through development of drone imaging technologies. In addition, numerous software solutions have become available for automated photogrammetric processing of aerial imaging materials. Numerous software developers, including the market leaders, are featuring products for photogrammetric image processing, such as PHOTOMOD, Envi, TerraSolid. The operating principle of automatic photogrammetric processing consists in the following. Information about each image is recorded in EXIF-file (imaging elevation, camera angle, exact longitude and latitude values). The software uses computer vision and photogrammetry technologies to locate common points in numerous images. Considering the geodata and camera angle, a color reference is found for each pixel in other images. Each coincidence becomes a key point. If a key point is found in at least three images, the software plots that image in space. The more key points are identified, the easier it is to determine spatial coordinates of the point. This stipulates the key rule – large image overlap is required. Software developers recommend overlap from 60 to 80%. Spatial coordinates of a point are obtained through triangulation method: a line of sight or ray is automatically traced from each imaging point to the selected point; and the intersection of these lines produces the target value.

This technology allows to obtain DOPMs, digital area/terrain models, 3D area models. In open terrain, the accuracy of data obtained through automatic photogrammetric image processing is comparable to that of laser scanning.

Let us review in detail these two technologies of producing a "points cloud", from the point of view of final consumers – data producers. Cost, Quality and Time were selected at comparison criteria.

1) In terms of data acquisition cost

Automatic photogrammetric image processing technology is viewed as a cheaper alternative to ALS and DAP. Densely populated point clouds may be obtained in addition to laser reflection points, if a digital camera is added to the aircraft equipment set. However, imaging performed with a drone, which can be rather moderately priced, considerably reduces the cost of works associated with acquisition of digital area model. Laser scanning data acquisition technology requires a much more extensive budget due to high lidar rent/purchase and service costs as well as expensive aircraft lease (purchase).

2) In terms of data quality

The technology of automatic photogrammetric image processing does not enable acquisition of high-quality data in wooded areas, in territories with tall vegetation, which is due to the nature of data processing technology. Additional field measurements are required to refine the digital terrain model in obscured territories (Fig. 1).

It is apparent in the image below that automatic photogrammetric image processing technology, as opposed to ALS, fails to obtain information about terrain under vegetation.

By means of the next step of comparison, let us review the density of point clouds obtained with a laser scanner vs. "photogrammetric clouds". Density of the former is several times lower than that of clouds obtained with photogrammetric methods (Table 1). However, at the same time, "laser point clouds" provide a much more uniform description of the object (Fig. 2), which is also apparent from the points density. In different

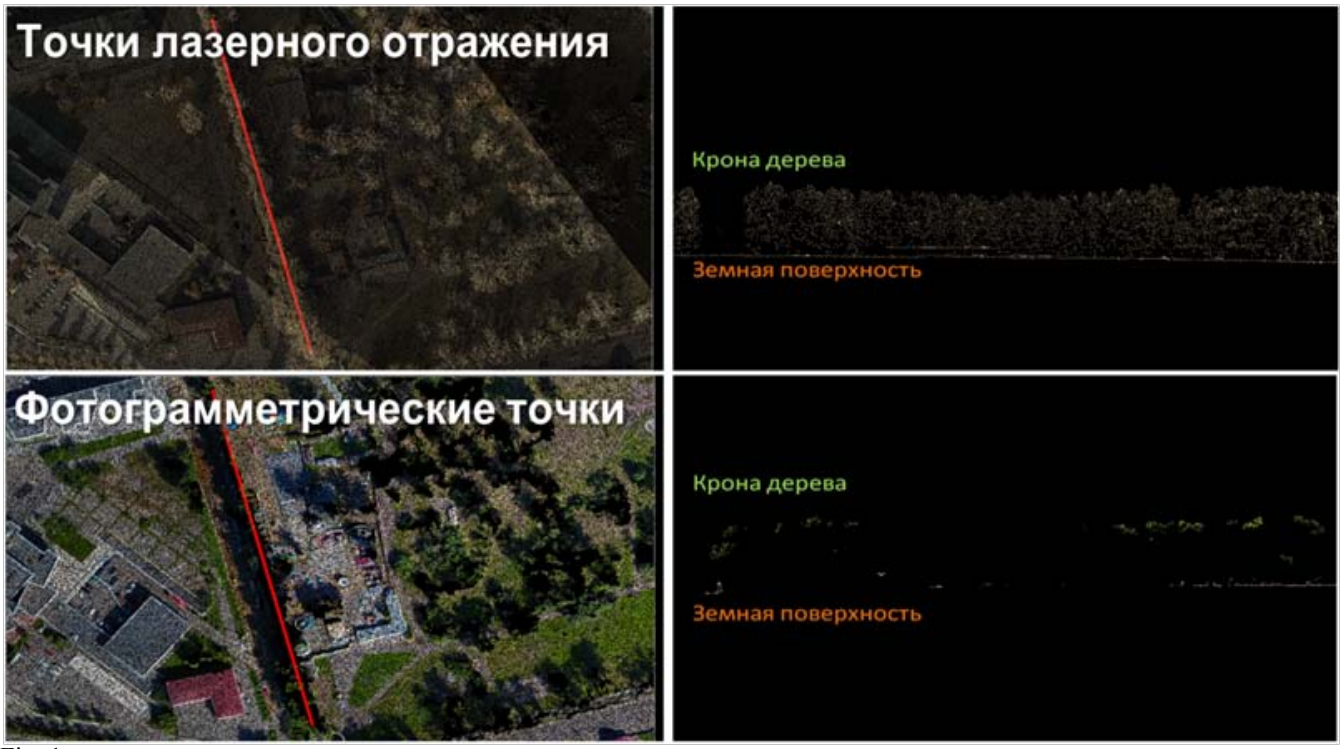

Fig. 1

areas of the test object, density based on automatic photogrammetric image processing can be different, which indicates at irregularity of data coverage.

Plane and elevation parameters of point cloud and digital orthophotomaps produced on their basis are comparable in accuracy (Table 2), which can be claimed after comparison of DAMs obtained with different methods vs. the tacheometric survey in a reference terrain area. Both methods meet the requirements to produce a digital topographic product in scale 1:500.

Object	Laser reflection points density, per 1 m^2	Automatic photogrammetric points density, per 1 m^2
Irkutsk City, Nizhnyaya Naberezhnaya St.	26-30	10-1700

Table 1

Object	Laser reflection points accuracy		Automatic photogrammetric points accuracy	
Irkutsk City, Block 130	Plane, m	Elevation, m	Plane, m	Elevation, m
	0.07	0.04	0.06	0.09

Table 2

Fig. 2

DOPMs plotted using automatic photogrammetric image processing technology contain numerous "artefacts" associated with elevated objects, which affect the coordinates measurement accuracy and appear less attractive (Fig. 3).

Fig. 3

3) In terms of data processing time

All software products for acquisition of photogrammetric point clouds work with virtually no involvement of the operator, in automatic mode, and their processing speed is limited by the computational capacity of the workstation used for processing. The operator is only required to verify operations at each stage and, if processing is performed using a ground reference, the data processing operator is only required to "pinpoint" the reference correctly. The amount of human-factor related errors is reduced using this approach. On the contrary, ALS and DAP technology requires a lot of attention, including calculation correct flightpath with streamlining by inertial system, downloading of laser reflection points and their correct calibration, digital image camera calibration and manual classification of points, all of which require lots of time resources.

Consolidating the above, the following conclusions may be derived: both technologies yield the stated accuracy requirements and are suitable for small-scale area mapping. Meanwhile, automatic photogrammetric image processing technology appears to be less expensive than laser scanning technology, drone-based acquisition of photogrammetric clouds is suitable for local, unobstructed areas of terrain, such as quarries or small settlements.

At the current level of development of geoinformation services, ALS and DAP technologies constitute the most attractive alternative in remote geodata coverage, as they enable to acquire spatial data over larger areas, densely developed territories and wooded terrain, which are especially typical for vasts spaces of Russia.

Sponsors

Silver Sponsors:

DigitalGlobe (USA)

SI Imaging Services (Korea)

National Company «Kazakhstan Gharysh Sapary» (Kazakhstan)

Media partners

Contacts

Racurs Co.
13A, Yaroslavskaya Str., Moscow, 129366, Russia
Tel: +7 (495) 720-51-27
Fax: +7 (495) 720-51-28
conference@racurs.ru
http://conf.racurs.ru